BELM: Bidirectional Explicit Linear Multi-step Sampler for Exact Inversion in Diffusion Models

Fangyikang Wang[1*] **Hubery Yin**[2*] **Yuejiang Dong**[3] **Huminhao Zhu**[1]
Chao Zhang[1†] **Hanbin Zhao**[1] **Hui Qian**[1] **Chen Li**[2]
[1]Zhejiang University [2]WeChat, Tencent Inc. [3]Tsinghua University
{wangfangyikang,zhuhuminhao,zczju,zhaohanbin,qianhui}@zju.edu.cn
{hubery,chaselli}@tencent.com
dongyj21@mails.tsinghua.edu.cn

Abstract

The inversion of diffusion model sampling, which aims to find the corresponding initial noise of a sample, plays a critical role in various tasks. Recently, several heuristic exact inversion samplers have been proposed to address the inexact inversion issue in a training-free manner. However, the theoretical properties of these heuristic samplers remain unknown and they often exhibit mediocre sampling quality. In this paper, we introduce a generic formulation, *Bidirectional Explicit Linear Multi-step* (BELM) samplers, of the exact inversion samplers, which includes all previously proposed heuristic exact inversion samplers as special cases. The BELM formulation is derived from the variable-stepsize-variable-formula linear multi-step method via integrating a bidirectional explicit constraint. We highlight this bidirectional explicit constraint is the key of mathematically exact inversion. We systematically investigate the Local Truncation Error (LTE) within the BELM framework and show that the existing heuristic designs of exact inversion samplers yield sub-optimal LTE. Consequently, we propose the Optimal BELM (O-BELM) sampler through the LTE minimization approach. We conduct additional analysis to substantiate the theoretical stability and global convergence property of the proposed optimal sampler. Comprehensive experiments demonstrate our O-BELM sampler establishes the exact inversion property while achieving high-quality sampling. Additional experiments in image editing and image interpolation highlight the extensive potential of applying O-BELM in varying applications.

1 Introduction

The emerging diffusion models (DMs) [52, 20, 55, 56], generating samples of data distribution from initial noise by learning a reverse diffusion process, have been proven to be an effective technique for modeling data distribution, especially in generating high-quality images [44, 10, 50, 46, 48, 21]. The diffusion process along with its sampling processes in DMs can be delineated as the forward and corresponding backward stochastic differential equations (SDE) [56, 1]. Furthermore, the sampling process can also be represented as a deterministic diffusion ordinary differential equation (ODE) [56, 53], which is also called Probability Flow ODE (PF-ODE) in some papers. Notably, the backward SDE and diffusion ODE share the same marginal distribution[56].

The inversion of the diffusion sampling, which aims to elucidate the correspondences between samples and initial noise, plays a critical role in various tasks of DMs. The diffusion inversion has

*Equal contribution. This work was done when Fangyikang Wang was an intern at WeChat.
†Corresponding author.

38th Conference on Neural Information Processing Systems (NeurIPS 2024).

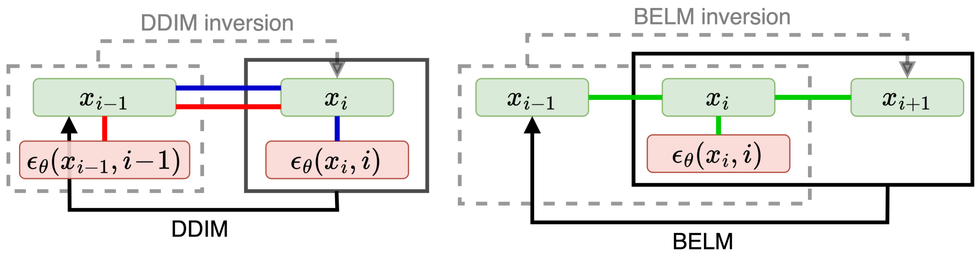

Figure 1: **Schematic description** of DDIM (left) and BELM (right). DDIM uses $\mathbf{x}_i$ and $\varepsilon_\theta(\mathbf{x}_i, i)$ to calculate $\mathbf{x}_{i-1}$ based on a linear relation between $\mathbf{x}_i$, $\mathbf{x}_{i-1}$ and $\varepsilon_\theta(\mathbf{x}_i, i)$ (represented by the blue line). However, DDIM inversion uses $\mathbf{x}_{i-1}$ and $\varepsilon_\theta(\mathbf{x}_{i-1}, i-1)$ to calculate $\mathbf{x}_i$ based on a different linear relation represented by the red line. This mismatch leads to the inexact inversion of DDIM. In contrast, BELM seeks to establish a linear relation between $\mathbf{x}_{i-1}$, $\mathbf{x}_i$, $\mathbf{x}_{i+1}$ and $\varepsilon_\theta(\mathbf{x}_i, i)$ (represented by the green line). BELM and its inversion are derived from this unitary relation, which facilitates the exact inversion. Specifically, BELM uses the linear combination of $\mathbf{x}_i$, $\mathbf{x}_{i+1}$ and $\varepsilon_\theta(\mathbf{x}_i, i)$ to calculate $\mathbf{x}_{i-1}$, and the BELM inversion uses the linear combination of $\mathbf{x}_{i-1}$, $\mathbf{x}_i$ and $\varepsilon_\theta(\mathbf{x}_i, i)$ to calculate $\mathbf{x}_{i+1}$. The bidirectional explicit constraint means this linear relation does not include the derivatives at the bidirectional endpoint, that is, $\varepsilon_\theta(\mathbf{x}_{i-1}, i-1)$ and $\varepsilon_\theta(\mathbf{x}_{i+1}, i+1)$.

a variety of downstream applications, including image editing [18, 57], image interpolation [53], inpainting [7], and super-resolution [67]. Several studies [31, 30, 7] have endeavored to tackle the inversion task within the context of SDE-based diffusion sampling. However, these works have not been able to achieve a mathematically exact inversion due to the inherent stochasticity of SDE.

In contrast, the diffusion ODE naturally gives out a correspondence between samples and noise. The famous DDIM [53] and its inversion are formulated by considering a first-order explicit Euler discretization to the diffusion ODE. However, as noted in the work of [18], the DDIM inversion introduces an inconsistency problem due to the schematic mismatch between DDIM and its inversion (see Figure 1). Encoding from x_0 to x_T using DDIM inversion and then decoding using DDIM often leads to inexact reconstructions of the original samples (see Figure 4). To enable exact inversion, the work of null-text inversion [42] introduces intensive training for iterative optimization but still falls short of achieving a mathematically exact inversion.

Recently, several heuristic exact inversion samplers have been proposed to address this inexact inversion issue in a training-free manner [63, 71]. These samplers enable the mathematically exact inversion without the need for additional training and are thus compatible with pre-trained models. Taking inspiration from affine coupling layers in normalizing flows [11, 12], EDICT [63] intuitively introduces an auxiliary diffusion state and performs alternating mixture updates on the primal and auxiliary diffusion states. Later, BDIA [71] employs a symmetric bidirectional integration structure to achieve exact inversion intuitively. However, these heuristic exact inversion samplers often compromise the sampling quality due to their intuitive formula design. They may also introduce undesirable extra computational overhead or non-robust hyperparameters.

In this paper, we develop a generic formula for the general exact inversion samplers, termed as Bidirectional Explicit Linear Multi-step (BELM) samplers. We demonstrate that all previously proposed heuristic exact inversion samplers are, in fact, special instances of BELM samplers. The concept of BELM originates from the observation of the mismatch between DDIM formula and its inversion formula. BELM is formulated by establishing an unifying relationship, from which both BELM and its inversion are derived. More specifically, the unifying relationship of BELM is constructed in a variable-stepsize-variable-formula (VSVF) linear multi-step manner, supplemented with an additional bidirectional explicit constraint to facilitate exact inversion.

We systematically investigate the Local Truncation Error (LTE) within the BELM framework and show that the existing heuristic designs of exact inversion samplers yield sub-optimal LTE. Consequently, we employed a LTE minimization approach to design the formula of the optimal case within BELM, which we refer to as O-BELM. The formula for O-BELM dynamically adjusts in accordance with the timesteps, thereby ensuring minimized local error and consequently yielding the highest possible sampling accuracy. Furthermore, we demonstrate that O-BELM possesses the desirable property of zero-stability, which makes O-BELM robust to initial values. It also has the beneficial property of global convergence, which prevents O-BELM from diverging during sampling. To the best of our knowledge, O-BELM is the first theoretically guaranteed exact inversion diffusion sampler.

We perform an image reconstruction experiment on the COCO dataset to validate that our O-BELM indeed achieves exact inversion, thereby enabling it to precisely recover complex image features. Furthermore, experiments involving both unconditional and conditional image generation demonstrate that O-BELM can ensure high sampling quality. Additional experiments in downstream tasks such as image editing and image interpolation highlight the extensive application potential of O-BELM.

2 Preliminaries

2.1 Diffusion Models and Diffusion SDEs

Suppose that we have a d-dimensional random variable $\mathbf{x}(0) \in \mathbb{R}^d$ following an unknown target distribution $q_0(x_0)$. Diffusion Models (DMs) define a forward process $\{\mathbf{x}(t)\}_{t\in[0,T]}$ with $T > 0$ starting with $\mathbf{x}(0)$, such that the distribution of $\mathbf{x}(t)$ conditioned on $\mathbf{x}(0)$ satisfies

$$q_{t|0}(\mathbf{x}(t)|\mathbf{x}(0)) = \mathcal{N}(\mathbf{x}(t); \alpha(t)\mathbf{x}(0), \sigma^2(t)\mathbf{I}), \tag{1}$$

where $\alpha(\cdot), \sigma(\cdot) \in \mathcal{C}([0,T], \mathbb{R}^+)$ have bounded derivatives, and we denote them as α_t and σ_t for simplicity. The choice for α_t and σ_t is referred to as the noise schedule of a DM. According to [33, 29, 38], with some assumption on $\alpha(\cdot)$ and $\sigma(\cdot)$, the forward process can be modeled as a linear SDE which is also called Ornstein–Uhlenbeck process:

$$\mathrm{d}\mathbf{x}(t) = f(t)\mathbf{x}(t)\mathrm{d}t + g(t)\mathrm{d}B_t, \tag{2}$$

where B_t is the standard d-dimensional Brownian Motion (BM), $f(t) = \frac{\mathrm{d}\log\alpha_t}{\mathrm{d}t}$ and $g^2(t) = \frac{\mathrm{d}\sigma_t^2}{\mathrm{d}t} - 2\frac{\mathrm{d}\log\alpha_t}{\mathrm{d}t}\sigma_t^2$. Under some regularity conditions, the above forward SDE (2) have a reverse SDE from time T to 0, which starts from $\mathbf{x}(t)$ [1]:

$$\mathrm{d}\mathbf{x}(t) = \left[f(t)\mathbf{x}(t) - g^2(t)\nabla_{\mathbf{x}(t)}\log q(\mathbf{x}(t), t)\right]\mathrm{d}t + g(t)\mathrm{d}\tilde{B}_t, \tag{3}$$

where $\tilde{B}_t$ is the reverse-time Brownian motion and $q(\mathbf{x}(t), t)$ is the single-time marginal distribution of the forward process. In practice, DMs [20, 56] use $\boldsymbol{\varepsilon}_\theta(\mathbf{x}(t), t)$ to estimate $-\sigma(t)\nabla_{\mathbf{x}(t)}\log q(\mathbf{x}(t), t)$ and the parameter θ is optimized by the following objective:

$$\theta^* = \arg\min_\theta \mathbb{E}_t\left\{\lambda_t \mathbb{E}_{x_0, x_t}\left[\|s_\theta(x_t, t) - \nabla_{x_t}\log p(x_t, t|x_0, 0)\|^2\right]\right\}, \tag{4}$$

2.2 Diffusion ODE and DDIM

It is noted that the reverse SDE (3) has an associated probability flow ODE (also called diffusion ODE), which is a deterministic process that shares the same single-time marginal distribution [56]:

$$\mathrm{d}\mathbf{x}(t) = \left[f(t)\mathbf{x}(t) - \frac{1}{2}g^2(t)\nabla_{\mathbf{x}(t)}\log q(\mathbf{x}(t), t)\right]\mathrm{d}t. \tag{5}$$

Upon substituting the $f(t)$ and $g(t)$ into Eq. (5), we obtain the following first-order form:

$$\mathrm{d}\left(\frac{\mathbf{x}(t)}{\alpha_t}\right) = \boldsymbol{\varepsilon}_\theta\left(\mathbf{x}(t), t\right)\mathrm{d}\left(\frac{\sigma_t}{\alpha_t}\right). \tag{6}$$

The famous DDIM sampler [53] can be obtained by applying the explicit Euler method to Eq. (6).

$$\mathbf{x}_{i-1} = \frac{\alpha_{i-1}}{\alpha_i}\mathbf{x}_i + \left(\sigma_{i-1} - \frac{\alpha_{i-1}}{\alpha_i}\sigma_i\right)\boldsymbol{\varepsilon}_\theta(\mathbf{x}_i, i). \tag{7}$$

The inversion of DDIM is obtained by applying the explicit Euler method in the reverse of Eq. (6):

$$\mathbf{x}_i = \frac{\alpha_i}{\alpha_{i-1}}\mathbf{x}_{i-1} + \left(\sigma_i - \frac{\alpha_i}{\alpha_{i-1}}\sigma_{i-1}\right)\boldsymbol{\varepsilon}_\theta(\mathbf{x}_{i-1}, i-1). \tag{8}$$

2.3 Intuitive Exact Inversion Samplers of Diffusion Models

In practice, we observe an inconsistency issue with the DDIM inversion (8). Consider a sample $\mathbf{x}_0$; using DDIM inversion, we obtain the corresponding noise $\mathbf{x}_T$ and then use DDIM to reconstruct a $\mathbf{x}_0^*$. The reconstructed $\mathbf{x}_0^*$ would exhibit significant inconsistency with the original sample $\mathbf{x}_0$. Recently, two exact inversion samplers, EDICT and BDIA, have been heuristically proposed to address this inconsistency issue in a training-free manner.

EDICT sampler Taking inspiration from affine coupling layers in normalizing flows [11, 12], the recent work [63] proposed EDICT to enforce exact diffusion inversion. The basic idea lies in introducing an auxiliary diffusion state $\mathbf{y}_t$ to be coupled with $\mathbf{x}_t$. Denoting $a_i = \frac{\alpha_{i-1}}{\alpha_i}$ and $b_i = \sigma_{i-1} - \frac{\alpha_{i-1}}{\alpha_i}\sigma_i$, the formulation of EDICT writes:

$$\begin{cases} \mathbf{x}_i^{inter} = a_i\mathbf{x}_i + b_i\boldsymbol{\varepsilon}_\theta(\mathbf{y}_i, i), & \mathbf{y}_i^{inter} = a_i\mathbf{y}_i + b_i\boldsymbol{\varepsilon}_\theta(\mathbf{x}(t)^{inter}, i), \\ \mathbf{x}_{i-1} = p\mathbf{x}_i^{inter} + (1-p)\mathbf{y}_i^{inter}, & \mathbf{y}_{i-1} = p\mathbf{y}_i^{inter} + (1-p)\mathbf{x}_{i-1}. \end{cases} \tag{9}$$

where $p \in (0, 1)$ is the mixing coefficient. The details of EDICT inversion defers to Appendix A.1.

BDIA sampler BDIA sampler [71] utilizes a symmetric bidirectional integration structure to achieve exact inversion. BDIA reformulate the expression of DDIM (7) to be $\mathbf{x}_{i-1}^{\text{DDIM}} = \mathbf{x}_i^{\text{DDIM}} + \Delta\left(i \to i-1|\mathbf{x}_i^{\text{DDIM}}\right)$ and the expression of DDIM inversion (8) to be $\mathbf{x}_i^{\text{DDIM}} = \mathbf{x}_{i-1}^{\text{DDIM}} + \Delta\left(i-1 \to i|\mathbf{x}_{i-1}^{\text{DDIM}}\right)$. BDIA intuitively leverage $-\left[(1-\gamma)(\mathbf{x}_{i+1} - \mathbf{x}_i) + \gamma\Delta\left(i \to i+1|\mathbf{x}_i\right)\right]$ to approximate the increment from x_{i+1} to x_i and $\Delta\left(i \to i-1|\mathbf{x}_i\right)$ as the increment from x_i to x_{i-1} . Thus, the updating rule of BDIA writes:

$$\mathbf{x}_{i-1} = \mathbf{x}_{i+1} \underbrace{- \left[(1-\gamma)(\mathbf{x}_{i+1} - \mathbf{x}_i) + \gamma\Delta\left(i \to i+1|\mathbf{x}_i\right)\right]}_{increment(\mathbf{x}_{i+1} \to \mathbf{x}_i)} + \underbrace{\Delta\left(i \to i-1|\mathbf{x}_i\right)}_{increment(\mathbf{x}_i \to \mathbf{x}_{i-1})} . \tag{10}$$

The comprehensive formulation of BDIA and its inversion can be found in Appendix A.2.

However, the theoretical properties of these heuristic samplers remain unknown and they often exhibit compromised sampling quality. To the best of our knowledge, there is no systematic approach to derive a diffusion sampler that simultaneously possesses the exact diffusion inversion property and maintains high sampling quality.

3 The Generic Bidirectional Explicit Linear Multi-step (BELM) Samplers

In this section, we first model the diffusion sampling process as a well-posed initial value problem to facilitate subsequent analysis. By the rethinking of DDIM inversion, we propose the generic Bidirectional Explicit Linear Multi-step (BELM) samplers in a variable-stepsize-variable-formula (VSVF) manner. We further illustrate that EDICT and BDIA are, in fact, special instances of the BELM framework.

The diffusion sampling problem as an IVP By denoting $\bar{\mathbf{x}}(t) \equiv \frac{\mathbf{x}(t)}{\alpha_t}$, $\bar{\sigma}(t) \equiv \frac{\sigma_t}{\alpha_t}$ and $\bar{\boldsymbol{\varepsilon}}_\theta(\bar{\mathbf{x}}(t), \bar{\sigma}_t) \equiv \boldsymbol{\varepsilon}_\theta\left(\mathbf{x}(t), t\right)$, the deterministic sampling process of DMs (6) can be seen as an special reverse-time diffusion initial value problem (IVP) [58, p.310][3, p.3]:

$$\mathrm{d}\bar{\mathbf{x}}(t) = \bar{\boldsymbol{\varepsilon}}_\theta\left(\bar{\mathbf{x}}(t), \bar{\sigma}_t\right)\mathrm{d}\bar{\sigma}_t, \tag{11}$$

where $\bar{\mathbf{x}}(T) = \mathbf{x}(T)/\alpha_T$. A fundamental question before any further analysis is whether the given diffusion IVP (11) admits any solution and, if so, whether this solution is unique. Firstly, we need to establish some regularity assumptions on our diffusion sampling problem (6).

Assumption 1. *$\boldsymbol{\varepsilon}_\theta(\mathbf{x}, t)$ is continuous w.r.t. t and Lipschitz continuous w.r.t. $\mathbf{x}$ with the Lipschitz constant $L_{\boldsymbol{\varepsilon}_\theta}$, which implies $\|\boldsymbol{\varepsilon}_\theta(\mathbf{x}_1, t) - \boldsymbol{\varepsilon}_\theta(\mathbf{x}_2, t)\|_2 \leq L_{\boldsymbol{\varepsilon}_\theta}\|\mathbf{x}_1 - \mathbf{x}_2\|_2$.*

The Assumption 1 is a common assumption of the noise predictor $\varepsilon_\theta(\mathbf{x}, t)$ in the DMs literature [54]. Under the condition of Assumption 1, we can confirm the diffusion IVP (11) is well-posed by a direct application of the existence and uniqueness theorem in the IVP theory [3, p. 23].

Proposition 1. *Under Assumption 1, there exists a unique solution to the diffusion IVP* (11).

In this paper, $\mathbf{x}(\cdot)$ denote the continuous solution, and $\mathbf{x}_i$ denote numerical approximations.

Rethinking on DDIM inversion As shown in Figure 1, DDIM (7) and its inversion (8) are derived based on different linear relationships. We highlight that this mismatch results in the inexact inversion of DDIM. Building on this observation, a natural idea is to construct the DDIM inversion based on the same linear relationships as the DDIM to eliminate this mismatch. Regrettably, DDIM is constructed on a relationship between $\mathbf{x}_i$, $\mathbf{x}_{i-1}$, and $\varepsilon_\theta(\mathbf{x}_i, i)$ (utilizes $\mathbf{x}_i$, and $\varepsilon_\theta(\mathbf{x}_i, i)$ to compute $\mathbf{x}_{i-1}$), which DDIM inversion cannot leverage to directly calculate $\mathbf{x}_i$, as $\varepsilon_\theta(\mathbf{x}_i, i)$ is also unknown in the DDIM inversion case. This relation is explicit for DDIM but implicit for DDIM inversion. It should be noted that implicit equations must be solved using iterative methods such as Newton's method [58, p. 19], which are time-consuming and can introduce numerical error in the context of DMs [23, 39].

To address this issue, we establish a new relationship between adjacent states and derivatives, which can be explicitly computed in both directions. Subsequently, we formulate both the sampler and its inversion based on this singular linear relationship to achieve exact inversion. This is the fundamental concept of BELM samplers.

Bidirectional Explicit Linear Multi-step (BELM) samplers In an attempt to establish a linear relationship between $\mathbf{x}_i$, $\mathbf{x}_{i-1}$, $\varepsilon_\theta(\mathbf{x}_i, i)$, and $\varepsilon_\theta(\mathbf{x}_{i-1}, i-1)$ that can be explicitly computed bidirectionally, we must exclude both $\varepsilon_\theta(\mathbf{x}_i, i)$ and $\varepsilon_\theta(\mathbf{x}_{i-1}, i-1)$. However, this exclusion results in a relationship that lacks sufficient information. Consequently, it becomes imperative to take more states into account. This prompts us to explore the concept of the linear multi-step (LM) method [3, p.111] as a means to derive a linear relationship between adjacent states and the derivatives of the diffusion IVP. However, the commonly used noise schedule of DMs would lead to a non-equidistant series of $\{\bar{\sigma}_i\}, i = 1 \dots N$. So, instead of the classical LM methods with fixed stepsize, we shall consider it in the variable-stepsize-variable-formula (VSVF) manner [8], which use dynamic multistep formulae w.r.t. different stepsizes. Let $t_0 < t_1 < \dots t_N = t_0 + T$ be a grid in $[t_0, t_0 + T]$, $h_i = \bar{\sigma}_i - \bar{\sigma}_{i-1}, i = N \dots 1, h_0 = \bar{\sigma}_0$ and $h = \max h_i$, the k-step VSVF LM methods w.r.t. Eq. (11) will calculate $\bar{\mathbf{x}}_{i-1}$ at the points $\bar{\sigma}_{i-1}$ with the following difference equation:

$$\bar{\mathbf{x}}_{i-1} = \sum_{j=1}^{k} a_{i,j} \cdot \bar{\mathbf{x}}_{i-1+j} + \sum_{j=0}^{k} b_{i,j} \cdot h_{i-1+j} \cdot \bar{\varepsilon}_\theta(\bar{\mathbf{x}}_{i-1+j}, \bar{\sigma}_{i-1+j}), \tag{12}$$

where the coefficient of updates and stepsizes are all dependent on i. Throughout this paper, any reference to LM will, by default, imply VSVF LM unless explicitly stated otherwise. If $b_{i,0} = 0$ for all i in Eq. (12), the method is called **explicit**, since the formula can directly compute $\bar{\mathbf{x}}_{i-1}$. Clearly, the LM (12) have a reversed formula which is also a k-step LM as follows (assume $a_{i,k} \neq 0$),

$$\bar{\mathbf{x}}_{i-1+k} = \frac{1}{a_{i,k}} \cdot \bar{\mathbf{x}}_{i-1} - \sum_{j=1}^{k-1} \frac{a_{i,j}}{a_{i,k}} \cdot \bar{\mathbf{x}}_{i-1+j} + \sum_{j=0}^{k} \frac{b_{i,j}}{a_{i,k}} \cdot h_{i-1+j} \cdot \bar{\varepsilon}_\theta(\bar{\mathbf{x}}_{i-1+j}, \bar{\sigma}_{i-1+j}). \tag{13}$$

If the reversed VSVFM is explicit, i.e. $b_{i,k} = 0$ for all i, we call the origin LM (12) to be **backward explicit**. Now we can define a k-step LM to be **bidirectional explicit** when it is explicit as well as backward explicit. We call the LM samplers abide by the bidirectional explicit constraint as the Bidirectional Explicit Linear Multi-step **(BELM)** samplers, which have the general form:

$$\bar{\mathbf{x}}_{i-1} = \sum_{j=1}^{k} a_{i,j} \cdot \bar{\mathbf{x}}_{i-1+j} + \sum_{j=1}^{k-1} b_{i,j} \cdot h_{i-1+j} \cdot \bar{\varepsilon}_\theta(\bar{\mathbf{x}}_{i-1+j}, \bar{\sigma}_{i-1+j}). \tag{14}$$

We highlight this bidirectional explicit constraint is key to mathematically exact diffusion inversion:

Proposition 2. *Any BELM method* (14) *with $a_{i,k} \neq 0$ has the exact inversion property.*

Table 1: Theoretical properties comparison of different samplers.

	Theoretical properties			
	exact inversion	local error	zero-stable	global convergence
DDIM[53]	✗	$\mathcal{O}\left(\alpha_i {h_i}^2\right)$	✓	✓
EDICT[63]	✓	$\mathcal{O}\left(\sqrt{\alpha_{i-1}} h_i\right)$	unclear	unclear
BDIA[71]	✓	$\mathcal{O}\left(\alpha_i (h_i + h_{i+1})^2\right)$	unclear	unclear
O-BELM (Ours)	✓	$\mathcal{O}\left(\alpha_i (h_i + h_{i+1})^3\right)$	✓	✓

As an instance, setting $k = 2$ in Eq. (14) yields the 2-step BELM diffusion sampler:

$$\bar{\mathbf{x}}_{i-1} = a_{i,2}\bar{\mathbf{x}}_{i+1} + a_{i,1}\bar{\mathbf{x}}_i + b_{i,1} h_i \bar{\boldsymbol{\varepsilon}}_\theta(\bar{\mathbf{x}}_i, \bar{\sigma}_i). \tag{15}$$

For detailed information on the 3-step BELM diffusion sampler, the general k-step case, and their optimal design, readers are referred to Appendix A.4 and A.5. In the main body of this paper, we will default mean 2-step case unless explicitly stated.

BDIA and EDICT as special case of BELM We find that, although developed from heuristic ideas, both BDIA and EDICT are special cases within the BELM framework. That is, their exact inversion property is inherited from the fact that they are fundamentally instances of BELM samplers.

Remark 1. *EDICT* (9) *and BDIA* (10) *are both special cases within the BELM framework.*

The detailed mathematical derivation for Remark 1 can be found in Appendices A.7 and A.8.

4 The Optimal-BELM (O-BELM) Sampler

In this section, we systematically investigate the Local Truncation Error (LTE) within the BELM framework and show that the existing heuristic designs of exact inversion samplers yield sub-optimal LTE. Consequently, we introduce Optimal-BELM (O-BELM), which utilizes a more refined dynamic formula developed through the LTE minimization approach. Additional analysis is conducted to substantiate the theoretical stability and global convergence property of O-BELM.

4.1 Analysis on Local Truncation Error

The Local Truncation Error (LTE) quantifies the error introduced in a step update. Specifically, it computes the difference between the numerical solution and its underlying true solution, assuming perfect knowledge of the true solution at the previous states.

Definition 1. *The LTE of BELM* (15) *on $\bar{\mathbf{x}}_i$ at each step i is defined as :*

$$\tau_i = \bar{\mathbf{x}}(t_{i-1}) - a_{i,2}\bar{\mathbf{x}}_{i+1} - a_{i,1}\bar{\mathbf{x}}_i - b_{i,1} h_i \bar{\boldsymbol{\varepsilon}}_\theta(\bar{\mathbf{x}}_i, \bar{\sigma}_i). \tag{16}$$

Under Assumption 2 (details in Appendix A.3), we can utilize the Taylor expansion to investigate the LTE of BELM (15) as follows:

Proposition 3. *Under Assumption 2, the LTE of the BELM* (15) *gives general form as follows:*

$$\tau_i = c_{i,1}\bar{\mathbf{x}}(t_{i-1}) + c_{i,2}\bar{\boldsymbol{\varepsilon}}_\theta\left(\bar{\mathbf{x}}(t_{i-1}), \bar{\sigma}_{i-1}\right) + c_{i,3}\nabla_{\bar{\sigma}_{i-1}}\bar{\boldsymbol{\varepsilon}}_\theta\left(\bar{\mathbf{x}}(t_{i-1}), \bar{\sigma}_{i-1}\right) + \mathcal{O}\left((h_i + h_{i+1})^3\right), \tag{17}$$

where $c_{i,1} = 1 - a_{i,1} - a_{i,2}$, $c_{i,2} = -a_{i,1}h_i - a_{i,2}\left(h_i + h_{i+1}\right) - b_{i,1}h_i$, *and* $c_{i,3} = -\frac{a_{i,1}}{2}h_i^2 - \frac{a_{i,2}}{2}(h_i + h_{i+1})^2 - b_{i,1}h_i^2$.

In the task of DMs, our primary concern is the LTE on $\mathbf{x}_{i-1}$ rather than $\bar{\mathbf{x}}_{i-1}$. We denote the LTE on $\mathbf{x}_i$ as $\mathbf{e}_i$. It is clear that $\mathbf{e}_i = \alpha_{i-1}\tau_i$. We investigate the LTE of existing samplers as follows:

Corollary 1. *Under Assumption 2, the LTE $\mathbf{e}_i$ of DDIM sampler* (7) *is* $\mathcal{O}\left(\alpha_{i-1}{h_i}^2\right)$*; The LTE $\mathbf{e}_i$ of BDIA sampler* (10) *is* $\mathcal{O}\left(\alpha_{i-1}(h_i+h_{i+1})^2\right)$ *for any fixed* $\gamma \in [0,1]$*; The LTE $\mathbf{e}_i$ of EDICT sampler* (9) *is* $\mathcal{O}\left(\sqrt{\alpha_{i-1}}h_i\right)$ *for any constant* $p \in (0,1)$.

4.2 Optimal BELM Sampler via LTE Minimization

We then demonstrate that, through a meticulous design of formulae, we can achieve a higher order of LTE within the BELM framework compared to existing sub-optimal instances. Specifically, we utilize an LTE minimization approach, inspired by the design of renowned LM methods such as the Adams–Bashforth methods [2] or the Adams–Moulton methods [43, 40].

Proposition 4. *Under Assumption 2, the LTE τ_i of BELM diffusion sampler* (15) *can be accurate up to* $\mathcal{O}\left((h_i+h_{i+1})^3\right)$ *when formulae are designed as* $a_{i,1} = \frac{h_{i+1}^2-h_i^2}{h_{i+1}^2}$,$a_{i,2} = \frac{h_i^2}{h_{i+1}^2}$,$b_{i,1} = -\frac{h_i+h_{i+1}}{h_{i+1}}$.

When this is satisfied, obviously, the LTE $\mathbf{e}_i$ on $\mathbf{x}_{i-1}$ is $\mathcal{O}\left(\alpha_{i-1}(h_i+h_{i+1})^3\right)$. Substituting the designed formulas into (15), we derive the Optimal-BELM (O-BELM) sampler:

$$\mathbf{x}_{i-1} = \frac{h_i^2}{h_{i+1}^2}\frac{\alpha_{i-1}}{\alpha_{i+1}}\mathbf{x}_{i+1} + \frac{h_{i+1}^2-h_i^2}{h_{i+1}^2}\frac{\alpha_{i-1}}{\alpha_i}\mathbf{x}_i - \frac{h_i(h_i+h_{i+1})}{h_{i+1}}\alpha_{i-1}\boldsymbol{\varepsilon}_\theta(\mathbf{x}_i, i). \tag{18}$$

The inversion of O-BELM diffusion sampler (18) writes:

$$\mathbf{x}_{i+1} = \frac{h_{i+1}^2}{h_i^2}\frac{\alpha_{i+1}}{\alpha_{i-1}}\mathbf{x}_{i-1} + \frac{h_i^2-h_{i+1}^2}{h_i^2}\frac{\alpha_{i+1}}{\alpha_i}\mathbf{x}_i + \frac{h_{i+1}(h_i+h_{i+1})}{h_i}\alpha_{i+1}\boldsymbol{\varepsilon}_\theta(\mathbf{x}_i, i). \tag{19}$$

4.3 Further Theoretical Analysis on O-BELM

Here, we further demonstrate that the O-BELM not only surpasses in terms of local accuracy but also excels in **stability** and **global convergence** properties.

As is clear from (15), we need starting values before we can apply a method to the diffusion IVP. Of these, the initial one is given by the initial condition, but the others, have to be computed by other means, say, by using DDIM. At any rate, the starting values will contain numerical errors and it is crucial to ensure that perturbations of the initial values do not lead to an error explosion in the subsequent steps. This concept is encapsulated in numerical analysis as zero-stability.

Definition 2. *The LM* (12) *is said to be* ***zero-stable*** *if there exists a constant K such that, for any two sequences $\{\bar{\mathbf{x}}_i\}$ and $\{\bar{\mathbf{z}}_i\}$ that have been generated by the same formulae but different starting values $\bar{\mathbf{x}}_N, \bar{\mathbf{x}}_{N-1}, \ldots, \bar{\mathbf{x}}_{N-k+1}$ and $\bar{\mathbf{z}}_N, \bar{\mathbf{z}}_{N-1}, \ldots, \bar{\mathbf{z}}_{N-k+1}$, respectively, we have*

$$\|\bar{\mathbf{x}}_i - \bar{\mathbf{z}}_i\| \le K \max\left\{\|\bar{\mathbf{x}}_N - \bar{\mathbf{z}}_N\|, \|\bar{\mathbf{x}}_{N-1} - \bar{\mathbf{z}}_{N-1}\|, \ldots, \|\bar{\mathbf{x}}_{N-k+1} - \bar{\mathbf{z}}_{N-k+1}\|\right\}, \tag{20}$$

for all i, and as h tends to 0.

We also want to ensure that a method will gradually converge to the underlying truth as the stepsizes decrease, a concept that aligns with the global convergence property.

Definition 3. *The LM* (12) *is* ***globally convergent*** *if for every solution $\bar{\mathbf{x}}(t)$ of* (11)

$$\lim_{h\to 0}\max_{0\le i\le N}\|\bar{\mathbf{x}}_i - \bar{\mathbf{x}}(t_i)\| = 0, \tag{21}$$

when initial error $\sum_{j=N}^{N-1+k}\left(\|\bar{\mathbf{x}}_j - \bar{\mathbf{x}}(t_j)\| + h_i\|\bar{\boldsymbol{\varepsilon}}_\theta(\bar{\mathbf{x}}_j, \bar{\sigma}_j) - \bar{\boldsymbol{\varepsilon}}_\theta(\bar{\mathbf{x}}(t_j), \bar{\sigma}_j)\|\right)$ *tends to zero.*

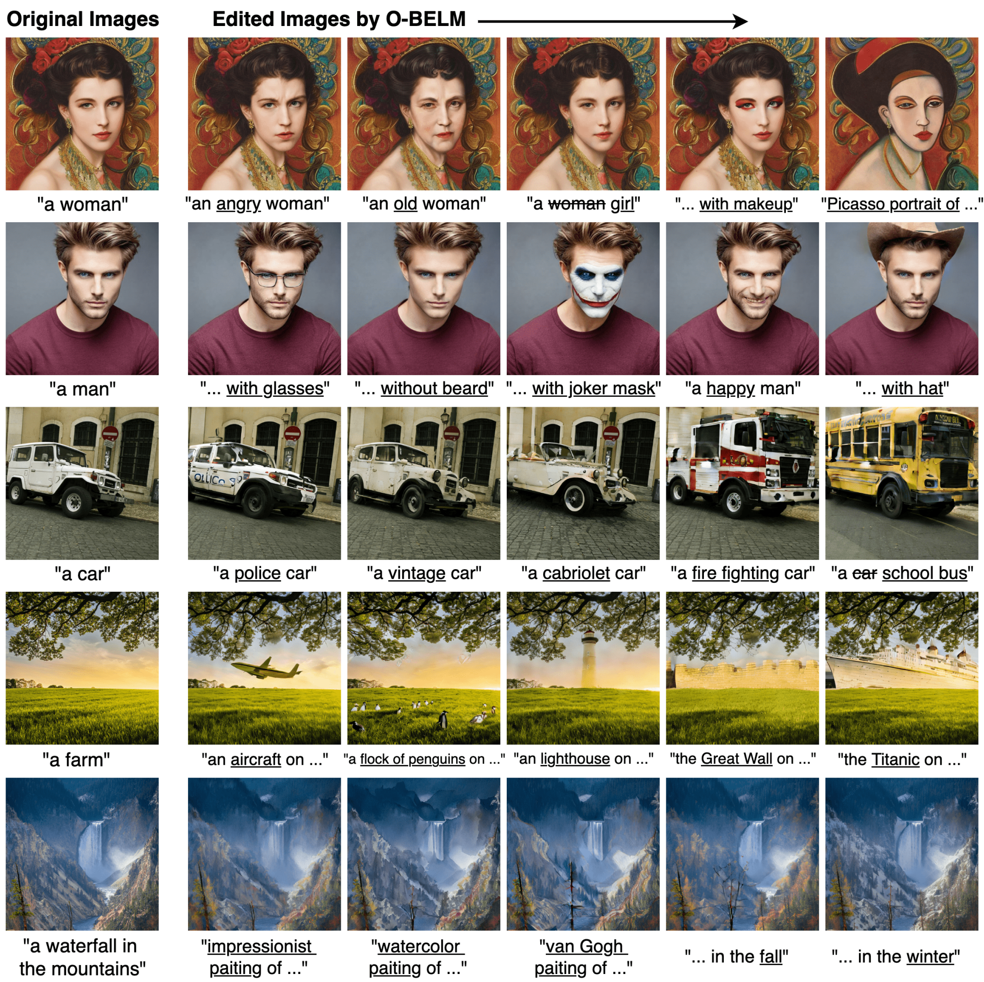

Figure 2: Examples of editing results using O-BELM on both synthesized and real images. We showcase the diverse editing capabilities of O-BELM across a range of tasks, including human face modifications, content change, entity addition and global style transfer. The exact inversion property of O-BELM enables large-scale image alterations while preserving auxiliary details (background in first row, hairstyle in second row, traffic sign in third row, tree and crop in fourth row, composition in last row). Its stability and accuracy further ensure the high quality of the resulting images.

We affirm that our O-BELM sampler possesses the nice zero-stable property as well as the global convergence property.

Proposition 5. *The O-BELM sampler* (18) *is (a)* ***zero-stable*** *and (b)* ***globally convergent****.*

5 Experiments

In this section, we conduct experiments to verify that O-BELM achieves the exact inversion property while maintaining high-quality sampling ability. We further demonstrate the extensive potential of applying the O-BELM sampler in various applications, such as image editing and image interpolation (deferred to Appendix C.3). All the pre-trained models utilized are listed in Appendix C.5.

5.1 Image Reconstruction

We adopt the experimental setting from [63] to demonstrate the exact diffusion inversion property of O-BELM using 10k images in the MS-COCO-2014 validation set [35]. Given an image, inverted latents are calculated and used to reconstruct the image using SD-1.5. Mean-square error (MSE) is calculated on pixels normalized to $[-1, 1]$ and averaged across 10k images. The autoencoder (AE)

Table 2: Comparison of different samplers on MSE reconstruction loss on COCO-14.

	MSE loss of reconstruction				
	DDIM	AE	EDICT	BDIA	**O-BELM**
10 steps	0.026	0.004	0.004	0.004	0.004
20 steps	0.016	0.004	0.004	0.004	0.004
50 steps	0.008	0.004	0.004	0.004	0.004
100 steps	0.007	0.004	0.004	0.004	0.004

Table 3: Comparison of different samplers on FID score($\downarrow$) for the task of unconditional generation.

	CIFAR10 (32 $\times$ 32)				CelebA-HQ (256 $\times$ 256)			
	DDIM	EDICT	BDIA	**O-BELM**	DDIM	EDICT	BDIA	**O-BELM**
10 steps	17.45	87.11	12.27	**10.98**	27.13	57.82	27.41	**19.13**
20 steps	10.60	38.84	**7.27**	**7.17**	16.33	39.24	16.18	**11.54**
50 steps	6.96	10.24	5.77	**5.24**	**10.77**	16.72	**10.65**	**10.41**
100 steps	5.72	5.31	5.07	**4.18**	**10.19**	12.24	**10.30**	**10.17**

reconstruction error in the SD pipeline serves as a lower bound. From Table 2, we observe that, regardless of the stepsize, O-BELM and its sub-optimal siblings BDIA and EDICT consistently achieve the lowest MSE, signifying their exact inversion at the latent level. In contrast, DDIM tends to suffer from inconsistency. More visual reconstruction examples can be found in Appendix C.1.

5.2 Unconditional Image Generation

In this section, we conduct an unconditional image generation task to validate the high-quality sampling ability of O-BELM. Utilizing a pre-trained model, we generate 50k artificial images over a specific number of steps and compute the corresponding Fréchet Inception Distance (FID) score with the real data. Specifically, Fréchet Inception Distance (FID) [19] calculates the Fréchet distance between the real data and the generated data. A lower FID implies more realistic generated data. Table 3 summarizes the computed FID scores for the CIFAR10 and CelebA-HQ datasets. It is evident that O-BELM consistently outperforms other exact inversion samplers in terms of sampling quality. This experimental result corroborates the error analysis presented in Table 1. The parameters γ for BDIA and p for EDICT are determined through grid search. Details can be found in Appendix C.2.

5.3 Conditional Image Generation

We further evaluate these samplers under conditional image generation tasks. We employ the StableDiffusion V1.5 and V2-base models to generate 30k images of resolution 512$\times$512, based on text prompts from the COCO-14 validation set. All methods utilize the same seed and the same text prompts set. As evident from Table 4, O-BELM also exhibits superior sampling quality in the context of conditional image generation. We ensure a fair comparison by selecting appropriate guidance weights and hyperparameters, details of which can be found in Appendix C.2.

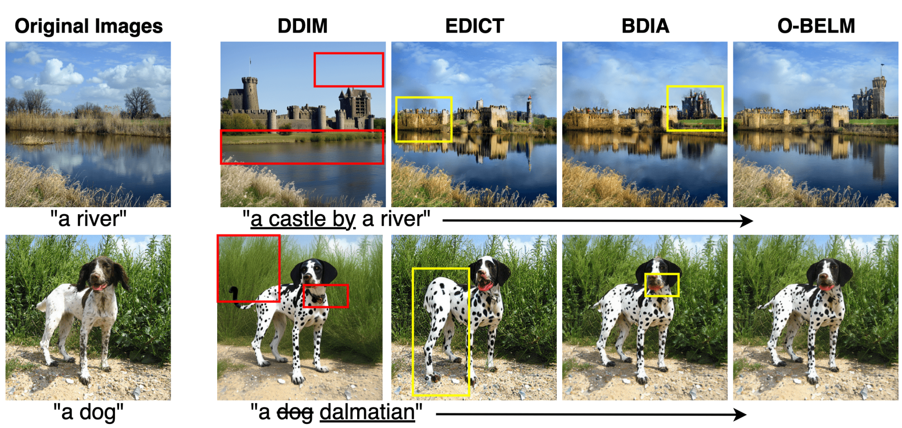

Figure 3: Comparison of editing results from different samplers under 50 steps. DDIM leads to inconsistencies (highlighted by the red rectangle), and the EDICT and BDIA samplers may introduce unrealistically low-quality sections (highlighted by the yellow rectangle). Our O-BELM sampler ensures consistency and demonstrates high-quality results.

Table 4: Comparison of different samplers on FID score($\downarrow$) for the task of text-to-image generation with pretrained stable diffusion models.

	SD-1.5 (512 $\times$ 512)				SD-2.0-base (512 $\times$ 512)			
	DDIM	EDICT	BDIA	**O-BELM**	DDIM	EDICT	BDIA	**O-BELM**
10 steps	21.44	85.77	23.96	**18.19**	20.40	75.14	22.00	**17.01**
20 steps	19.45	27.17	20.39	**17.92**	18.57	24.15	18.72	**16.53**
50 steps	18.93	21.30	19.38	**17.96**	17.82	19.76	17.98	**16.52**
100 steps	18.83	21.13	19.21	**18.19**	17.64	19.49	17.86	**16.75**

5.4 Training-free Image Editing

In this section, we present the results of the O-BELM sampler in an image editing task as shown in Figure 2, and compare the editing effects of different samplers in Figure 3. We demonstrate that the exact inversion property of O-BELM ensures the preservation of image features that we do not wish to edit. Furthermore, we illustrate how the high accuracy and stability properties of O-BELM contribute to the high quality of the edited image.

We emphasis that the goal of experiments here is not going to use our O-BELM sampler alone to achieve commercial-grade level image editing. It's quite unfair for training-free exact sampler methods to compete with commercial-grade image editing pipelines involving domain-specific training [25, 68], attention modification [18, 45], testing-time finetuning [62, 24, 6], complex control [73], real-data inversion alignment [75] or input text refinement [47, 37, 32]. In fact, our O-BELM sampler is orthogonal to these image editing techniques, using a better exact inversion sampler like O-BELM in the commercial-grade image editing pipeline remains a promising future work.

6 Conclusions

We tackle the inexact inversion issue of DMs in a training-free manner. We introduce the generic Bidirectional Explicit Linear Multi-step (BELM) framework based on a linear multi-step observation, which encompasses existing heuristic exact inversion samplers as special cases. Furthermore, we devise a Local Truncation Error (LTE) minimization approach to construct the Optimal-BELM (O-BELM) within the BELM framework, which achieves a higher order of local error. We provide a theoretical guarantee of global stability and convergence for O-BELM and conduct various experiments to demonstrate that O-BELM not only accomplishes exact inversion but also maintains a high-quality sampling capability. Please refer to further discussion and limitations in appendix D. The code repository can be found at `https://github.com/zituitui/BELM`.

7 Acknowledgments

This work was supported in part by National Natural Science Foundation of China under Grant 62206248 and National Natural Science Foundation of China under Grant 62402430. We would like to thank all the reviewers for their constructive comments. Fangyikang Wang wishes to express gratitude to Pengze Zhang from ByteDance, as well as Yiling Zhang and Yinan Li from Zhejiang University, for their insightful discussions on the experiments.

References

[1] Brian DO Anderson. Reverse-time diffusion equation models. *Stochastic Processes and their Applications*, 12(3):313–326, 1982.

[2] Francis Bashforth and John Couch Adams. *An attempt to test the theories of capillary action by comparing the theoretical and measured forms of drops of fluid*. University Press, 1883.

[3] John Charles Butcher. *Numerical methods for ordinary differential equations*. John Wiley & Sons, 2016.

[4] Zhichao Chen, Haoxuan Li, Fangyikang Wang, Odin Zhang, Hu Xu, Xiaoyu Jiang, Zhihuan Song, and Eric H Wang. Rethinking the diffusion models for numerical tabular data imputation from the perspective of wasserstein gradient flow. *arXiv preprint arXiv:2406.15762*, 2024.

[5] Hansam Cho, Jonghyun Lee, Seoung Bum Kim, Tae-Hyun Oh, and Yonghyun Jeong. Noise map guidance: Inversion with spatial context for real image editing. *arXiv preprint arXiv:2402.04625*, 2024.

[6] Jooyoung Choi, Yunjey Choi, Yunji Kim, Junho Kim, and Sungroh Yoon. Custom-edit: Text-guided image editing with customized diffusion models. *arXiv preprint arXiv:2305.15779*, 2023.

[7] Hyungjin Chung, Byeongsu Sim, Dohoon Ryu, and Jong Chul Ye. Improving diffusion models for inverse problems using manifold constraints. *Advances in Neural Information Processing Systems*, 35:25683–25696, 2022.

[8] M Crouzeix and FJ Lisbona. The convergence of variable-stepsize, variable-formula, multistep methods. *SIAM journal on numerical analysis*, 21(3):512–534, 1984.

[9] Germund Dahlquist. Convergence and stability in the numerical integration of ordinary differential equations. *Mathematica Scandinavica*, pages 33–53, 1956.

[10] Prafulla Dhariwal and Alexander Nichol. Diffusion models beat gans on image synthesis. In *Advances in Neural Information Processing Systems*, volume 34, pages 8780–8794, 2021.

[11] Laurent Dinh, David Krueger, and Yoshua Bengio. Nice: Non-linear independent components estimation. *arXiv preprint arXiv:1410.8516*, 2014.

[12] Laurent Dinh, Jascha Sohl-Dickstein, and Samy Bengio. Density estimation using real nvp. *arXiv preprint arXiv:1605.08803*, 2016.

[13] Jiahua Dong, Wenqi Liang, Hongliu Li, Duzhen Zhang, Meng Cao, Henghui Ding, Salman Khan, and Fahad Khan. How to continually adapt text-to-image diffusion models for flexible customization? In *Advances in Neural Information Processing Systems*, 2024.

[14] Qian Feng, Hanbin Zhao, Chao Zhang, Jiahua Dong, Henghui Ding, Yu-Gang Jiang, and Hui Qian. Pectp: Parameter-efficient cross-task prompts for incremental vision transformer. *arXiv preprint arXiv:2407.03813*, 2024.

[15] Qian Feng, Dawei Zhou, Hanbin Zhao, Chao Zhang, and Hui Qian. Lw2g: Learning whether to grow for prompt-based continual learning. *arXiv preprint arXiv:2409.18860*, 2024.

[16] Daniel Garibi, Or Patashnik, Andrey Voynov, Hadar Averbuch-Elor, and Daniel Cohen-Or. Renoise: Real image inversion through iterative noising. *arXiv preprint arXiv:2403.14602*, 2024.

[17] Ligong Han, Song Wen, Qi Chen, Zhixing Zhang, Kunpeng Song, Mengwei Ren, Ruijiang Gao, Anastasis Stathopoulos, Xiaoxiao He, Yuxiao Chen, et al. Proxedit: Improving tuning-free real image editing with proximal guidance. In *Proceedings of the IEEE/CVF Winter Conference on Applications of Computer Vision*, pages 4291–4301, 2024.

[18] Amir Hertz, Ron Mokady, Jay Tenenbaum, Kfir Aberman, Yael Pritch, and Daniel Cohen-or. Prompt-to-prompt image editing with cross-attention control. In *International Conference on Learning Representations*, 2023.

[19] Martin Heusel, Hubert Ramsauer, Thomas Unterthiner, Bernhard Nessler, and Sepp Hochreiter. Gans trained by a two time-scale update rule converge to a local nash equilibrium. *Advances in Neural Information Processing Systems (NeurIPS)*, 2017.

[20] Jonathan Ho, Ajay Jain, and Pieter Abbeel. Denoising diffusion probabilistic models. *Advances in Neural Information Processing Systems*, 33:6840–6851, 2020.

[21] Jonathan Ho, Chitwan Saharia, William Chan, David J. Fleet, Mohammad Norouzi, and Tim Salimans. Cascaded diffusion models for high fidelity image generation. *Journal of Machine Learning Research*, 23(47):1–33, 2022.

[22] Jonathan Ho and Tim Salimans. Classifier-free diffusion guidance. *arXiv preprint arXiv:2207.12598*, 2022.

[23] Seongmin Hong, Kyeonghyun Lee, Suh Yoon Jeon, Hyewon Bae, and Se Young Chun. On exact inversion of dpm-solvers. *arXiv preprint arXiv:2311.18387*, 2023.

[24] Jiancheng Huang, Yifan Liu, Jin Qin, and Shifeng Chen. Kv inversion: Kv embeddings learning for text-conditioned real image action editing. In *Chinese Conference on Pattern Recognition and Computer Vision (PRCV)*, pages 172–184. Springer, 2023.

[25] Nisha Huang, Yuxin Zhang, Fan Tang, Chongyang Ma, Haibin Huang, Weiming Dong, and Changsheng Xu. Diffstyler: Controllable dual diffusion for text-driven image stylization. *IEEE Transactions on Neural Networks and Learning Systems*, 2024.

[26] Inbar Huberman-Spiegelglas, Vladimir Kulikov, and Tomer Michaeli. An edit friendly ddpm noise space: Inversion and manipulations. *arXiv preprint arXiv:2304.06140*, 2023.

[27] The MathWorks Inc. Matlab version: 9.13.0 (r2022b), 2022.

[28] Xuan Ju, Ailing Zeng, Yuxuan Bian, Shaoteng Liu, and Qiang Xu. Direct inversion: Boosting diffusion-based editing with 3 lines of code. *arXiv preprint arXiv:2310.01506*, 2023.

[29] Tero Karras, Miika Aittala, Timo Aila, and Samuli Laine. Elucidating the design space of diffusion-based generative models. *arXiv preprint arXiv:2206.00364*, 2022.

[30] Bahjat Kawar, Michael Elad, Stefano Ermon, and Jiaming Song. Denoising diffusion restoration models. *Advances in Neural Information Processing Systems*, 35:23593–23606, 2022.

[31] Bahjat Kawar, Gregory Vaksman, and Michael Elad. Snips: Solving noisy inverse problems stochastically. *Advances in Neural Information Processing Systems*, 34:21757–21769, 2021.

[32] Sunwoo Kim, Wooseok Jang, Hyunsu Kim, Junho Kim, Yunjey Choi, Seungryong Kim, and Gayeong Lee. User-friendly image editing with minimal text input: Leveraging captioning and injection techniques. *arXiv preprint arXiv:2306.02717*, 2023.

[33] Diederik Kingma, Tim Salimans, Ben Poole, and Jonathan Ho. Variational diffusion models. In M. Ranzato, A. Beygelzimer, Y. Dauphin, P.S. Liang, and J. Wortman Vaughan, editors, *Advances in Neural Information Processing Systems*, volume 34, pages 21696–21707. Curran Associates, Inc., 2021.

[34] Liangchen Li and Jiajun He. Bidirectional consistency models. *arXiv preprint arXiv:2403.18035*, 2024.

[35] Tsung-Yi Lin, Michael Maire, Serge Belongie, James Hays, Pietro Perona, Deva Ramanan, Piotr Dollár, and C Lawrence Zitnick. Microsoft coco: Common objects in context. In *Computer Vision–ECCV 2014: 13th European Conference, Zurich, Switzerland, September 6-12, 2014, Proceedings, Part V 13*, pages 740–755. Springer, 2014.

[36] Yaron Lipman, Ricky TQ Chen, Heli Ben-Hamu, Maximilian Nickel, and Matt Le. Flow matching for generative modeling. *arXiv preprint arXiv:2210.02747*, 2022.

[37] Zhen Liu, Yao Feng, Michael J. Black, Derek Nowrouzezahrai, Liam Paull, and Weiyang Liu. Meshdiffusion: Score-based generative 3d mesh modeling. In *International Conference on Learning Representations*, 2023.

[38] Cheng Lu, Yuhao Zhou, Fan Bao, Jianfei Chen, Chongxuan Li, and Jun Zhu. Dpm-solver: A fast ode solver for diffusion probabilistic model sampling in around 10 steps. *Advances in Neural Information Processing Systems*, 35:5775–5787, 2022.

[39] Barak Meiri, Dvir Samuel, Nir Darshan, Gal Chechik, Shai Avidan, and Rami Ben-Ari. Fixed-point inversion for text-to-image diffusion models. *arXiv preprint arXiv:2312.12540*, 2023.

[40] William Edmund Milne. Numerical integration of ordinary differential equations. *The American Mathematical Monthly*, 33(9):455–460, 1926.

[41] Daiki Miyake, Akihiro Iohara, Yu Saito, and Toshiyuki Tanaka. Negative-prompt inversion: Fast image inversion for editing with text-guided diffusion models. *arXiv preprint arXiv:2305.16807*, 2023.

[42] Ron Mokady, Amir Hertz, Kfir Aberman, Yael Pritch, and Daniel Cohen-Or. Null-text inversion for editing real images using guided diffusion models. In *Proceedings of the IEEE/CVF Conference on Computer Vision and Pattern Recognition*, pages 6038–6047, 2023.

[43] Forest Ray Moulton. *New methods in exterior ballistics*. University of Chicago Press, 1926.

[44] Alexander Quinn Nichol, Prafulla Dhariwal, Aditya Ramesh, Pranav Shyam, Pamela Mishkin, Bob Mcgrew, Ilya Sutskever, and Mark Chen. GLIDE: Towards photorealistic image generation and editing with text-guided diffusion models. In *Proceedings of the 39th International Conference on Machine Learning*, volume 162, pages 16784–16804, 2022.

[45] Gaurav Parmar, Krishna Kumar Singh, Richard Zhang, Yijun Li, Jingwan Lu, and Jun-Yan Zhu. Zero-shot image-to-image translation. In *ACM SIGGRAPH 2023 Conference Proceedings*, pages 1–11, 2023.

[46] Aditya Ramesh, Prafulla Dhariwal, Alex Nichol, Casey Chu, and Mark Chen. Hierarchical text-conditional image generation with clip latents. *arXiv preprint arXiv:2204.06125*, 2022.

[47] Hareesh Ravi, Sachin Kelkar, Midhun Harikumar, and Ajinkya Kale. Preditor: Text guided image editing with diffusion prior. *arXiv preprint arXiv:2302.07979*, 2023.

[48] Robin Rombach, Andreas Blattmann, Dominik Lorenz, Patrick Esser, and Björn Ommer. High-resolution image synthesis with latent diffusion models. In *Proceedings of the IEEE/CVF Conference on Computer Vision and Pattern Recognition*, pages 10684–10695, 2022.

[49] Olaf Ronneberger, Philipp Fischer, and Thomas Brox. U-net: Convolutional networks for biomedical image segmentation. In *Medical image computing and computer-assisted intervention–MICCAI 2015: 18th international conference, Munich, Germany, October 5-9, 2015, proceedings, part III 18*, pages 234–241. Springer, 2015.

[50] Chitwan Saharia, William Chan, Saurabh Saxena, Lala Li, Jay Whang, Emily L Denton, Kamyar Ghasemipour, Raphael Gontijo Lopes, Burcu Karagol Ayan, Tim Salimans, Jonathan Ho, David J Fleet, and Mohammad Norouzi. Photorealistic text-to-image diffusion models with deep language understanding. In *Advances in Neural Information Processing Systems*, volume 35, pages 36479–36494, 2022.

[51] Ken Shoemake. Animating rotation with quaternion curves. In *Proceedings of the 12th annual conference on Computer graphics and interactive techniques*, pages 245–254, 1985.

[52] Jascha Sohl-Dickstein, Eric Weiss, Niru Maheswaranathan, and Surya Ganguli. Deep unsupervised learning using nonequilibrium thermodynamics. In *International Conference on Machine Learning*, pages 2256–2265. PMLR, 2015.

[53] Jiaming Song, Chenlin Meng, and Stefano Ermon. Denoising diffusion implicit models. In *International Conference on Learning Representations*, 2021.

[54] Yang Song, Prafulla Dhariwal, Mark Chen, and Ilya Sutskever. Consistency models. In *Proceedings of the 40th International Conference on Machine Learning*, ICML'23. JMLR.org, 2023.

[55] Yang Song and Stefano Ermon. Generative modeling by estimating gradients of the data distribution. *Advances in neural information processing systems*, 32, 2019.

[56] Yang Song, Jascha Sohl-Dickstein, Diederik P Kingma, Abhishek Kumar, Stefano Ermon, and Ben Poole. Score-based generative modeling through stochastic differential equations. *arXiv preprint arXiv:2011.13456*, 2020.

[57] Xuan Su, Jiaming Song, Chenlin Meng, and Stefano Ermon. Dual diffusion implicit bridges for image-to-image translation. *arXiv preprint arXiv:2203.08382*, 2022.

[58] Endre Süli and David F Mayers. *An introduction to numerical analysis*. Cambridge university press, 2003.

[59] Gan Sun, Wenqi Liang, Jiahua Dong, Jun Li, Zhengming Ding, and Yang Cong. Create your world: Lifelong text-to-image diffusion. *IEEE Transactions on Pattern Analysis and Machine Intelligence*, 46(9):6454–6470, 2024.

[60] Jiahang Tu, Hao Fu, Fengyu Yang, Hanbin Zhao, Chao Zhang, and Hui Qian. Texttoucher: Fine-grained text-to-touch generation. *arXiv preprint arXiv:2409.05427*, 2024.

[61] Jiahang Tu, Wei Ji, Hanbin Zhao, Chao Zhang, Roger Zimmermann, and Hui Qian. Driveditfit: Fine-tuning diffusion transformers for autonomous driving. *arXiv preprint arXiv:2407.15661*, 2024.

[62] Dani Valevski, Matan Kalman, Yossi Matias, and Yaniv Leviathan. Unitune: Text-driven image editing by fine tuning an image generation model on a single image. *arXiv preprint arXiv:2210.09477*, 2(3):5, 2022.

[63] Bram Wallace, Akash Gokul, and Nikhil Naik. Edict: Exact diffusion inversion via coupled transformations. In *Proceedings of the IEEE/CVF Conference on Computer Vision and Pattern Recognition*, pages 22532–22541, 2023.

[64] Boyang Wang, Fengyu Yang, Xihang Yu, Chao Zhang, and Hanbin Zhao. Apisr: Anime production inspired real-world anime super-resolution. In *Proceedings of the IEEE/CVF Conference on Computer Vision and Pattern Recognition*, pages 25574–25584, 2024.

[65] Fangyikang Wang, Huminhao Zhu, Chao Zhang, Hanbin Zhao, and Hui Qian. Gad-pvi: A general accelerated dynamic-weight particle-based variational inference framework. In *Proceedings of the AAAI Conference on Artificial Intelligence*, volume 38, pages 15466–15473, 2024.

[66] Hao Wang, Jiajun Fan, Zhichao Chen, Haoxuan Li, Weiming Liu, Tianqiao Liu, Quanyu Dai, Yichao Wang, Zhenhua Dong, and Ruiming Tang. Optimal transport for treatment effect estimation. *Advances in Neural Information Processing Systems*, 36:1–15, 2024.

[67] Xintao Wang, Ke Yu, Shixiang Wu, Jinjin Gu, Yihao Liu, Chao Dong, Yu Qiao, and Chen Change Loy. Esrgan: Enhanced super-resolution generative adversarial networks. In *Proceedings of the European conference on computer vision (ECCV) workshops*, pages 0–0, 2018.

[68] Zhizhong Wang, Lei Zhao, and Wei Xing. Stylediffusion: Controllable disentangled style transfer via diffusion models. In *Proceedings of the IEEE/CVF International Conference on Computer Vision*, pages 7677–7689, 2023.

[69] Andre Wibisono, Ashia C Wilson, and Michael I Jordan. A variational perspective on accelerated methods in optimization. *proceedings of the National Academy of Sciences*, 113(47):E7351–E7358, 2016.

[70] Duzhen Zhang, Yahan Yu, Jiahua Dong, Chenxing Li, Dan Su, Chenhui Chu, and Dong Yu. MM-LLMs: Recent advances in MultiModal large language models. In *Findings of the Association for Computational Linguistics ACL 2024*, pages 12401–12430, August 2024.

[71] Guoqiang Zhang, Jonathan P Lewis, and W Bastiaan Kleijn. Exact diffusion inversion via bi-directional integration approximation. *arXiv preprint arXiv:2307.10829*, 2023.

[72] Jiaxin Zhang, Kamalika Das, and Sricharan Kumar. On the robustness of diffusion inversion in image manipulation. In *ICLR 2023 Workshop on Trustworthy and Reliable Large-Scale Machine Learning Models*, 2023.

[73] Lvmin Zhang, Anyi Rao, and Maneesh Agrawala. Adding conditional control to text-to-image diffusion models. In *Proceedings of the IEEE/CVF International Conference on Computer Vision*, pages 3836–3847, 2023.

[74] Pengze Zhang, Hubery Yin, Chen Li, and Xiaohua Xie. Tackling the singularities at the endpoints of time intervals in diffusion models. *arXiv preprint arXiv:2403.08381*, 2024.

[75] Yuechen Zhang, Jinbo Xing, Eric Lo, and Jiaya Jia. Real-world image variation by aligning diffusion inversion chain. In A. Oh, T. Naumann, A. Globerson, K. Saenko, M. Hardt, and S. Levine, editors, *Advances in Neural Information Processing Systems*, volume 36, pages 30641–30661. Curran Associates, Inc., 2023.

[76] Huminhao Zhu, Fangyikang Wang, Chao Zhang, Hanbin Zhao, and Hui Qian. Neural sinkhorn gradient flow. *arXiv preprint arXiv:2401.14069*, 2024.

Appendix

Contents

A Formulations

A.1 Detail Formulation of EDICT

A sequential inversion and rearrangement of EDICT (9) yields the EDICT inversion:

$$\begin{cases} \mathbf{y}_i^{inter} = (\mathbf{y}_{i-1} - (1-p)\mathbf{x}_{i-1})/p, \\ \mathbf{x}_i^{inter} = (\mathbf{x}_{i-1} - (1-p)\mathbf{y}_i^{inter})/p, \\ \mathbf{y}_i = \left(\mathbf{y}_i^{inter} - b_i \boldsymbol{\varepsilon}_\theta(\mathbf{x}_i^{inter}, i)\right)/a_i, \\ \mathbf{x}_i = \left(\mathbf{x}_i^{inter} - b_i \boldsymbol{\varepsilon}_\theta(\mathbf{y}_i, i)\right)/a_i. \end{cases} \tag{22}$$

A.2 Detail Formulation of BDIA

BDIA sampler [71] utilizes bi-directional integration to achieve exact inversion, also introducing an additional hyperparameter. Reformulate the expression of DDIM (7) to be $\mathbf{x}_{i-1}^{\text{DDIM}} = \mathbf{x}_i^{\text{DDIM}} + \Delta\left(i \to i-1 | \mathbf{x}_i^{\text{DDIM}}\right)$ and the expression of DDIM inversion (8) to be $\mathbf{x}_i^{\text{DDIM}} = \mathbf{x}_{i-1}^{\text{DDIM}} + \Delta\left(i-1 \to i | \mathbf{x}_{i-1}^{\text{DDIM}}\right)$, that is,

$$\begin{cases} \Delta\left(i \to i-1 | \mathbf{x}_i\right) = \left(\frac{\alpha_{i-1}}{\alpha_i} - 1\right)\mathbf{x}_i + \left(\sigma_{i-1} - \frac{\alpha_{i-1}}{\alpha_i}\sigma_i\right)\boldsymbol{\varepsilon}_\theta(\mathbf{x}_i, i) \\ \Delta\left(i-1 \to i | \mathbf{x}_{i-1}\right) = \left(\frac{\alpha_i}{\alpha_{i-1}} - 1\right)\mathbf{x}_{i-1} + \left(\sigma_i - \frac{\alpha_i}{\alpha_{i-1}}\sigma_{i-1}\right)\boldsymbol{\varepsilon}_\theta(x_{i-1}, i-1). \end{cases} \tag{23}$$

The updating rule of BDIA write:

$$\begin{aligned} \mathbf{x}_{i-1} =& \mathbf{x}_{i+1} \underbrace{- \left[(1-\gamma)(\mathbf{x}_{i+1} - \mathbf{x}_i) + \gamma\Delta\left(i \to i+1 | \mathbf{x}_i\right)\right]}_{increment(\mathbf{x}_{i+1} \to \mathbf{x}_i)} + \underbrace{\Delta\left(i \to i-1 | \mathbf{x}_i\right)}_{increment(\mathbf{x}_i \to \mathbf{x}_{i-1})}, \\ =& \mathbf{x}_{i+1} - (1-\gamma)(\mathbf{x}_{i+1} - \mathbf{x}_i) - \gamma\left[\left(\frac{\alpha_{i+1}}{\alpha_i} - 1\right)\mathbf{x}_i + \left(\sigma_{i+1} - \frac{\alpha_{i+1}}{\alpha_i}\sigma_i\right)\boldsymbol{\varepsilon}_\theta(x_i, i)\right] \\ &+ \left[\left(\frac{\alpha_{i-1}}{\alpha_i} - 1\right)\mathbf{x}_i + \left(\sigma_{i-1} - \frac{\alpha_{i-1}}{\alpha_i}\sigma_i\right)\boldsymbol{\varepsilon}_\theta(\mathbf{x}_i, i)\right] \\ =& \gamma\mathbf{x}_{i+1} + \left(\frac{\alpha_{i-1}}{\alpha_i} - \gamma\frac{\alpha_{i+1}}{\alpha_i}\right)\mathbf{x}_i + \left[\sigma_{i-1} - \frac{\alpha_{i-1}}{\alpha_i}\sigma_i - \gamma\left(\sigma_{i+1} - \frac{\alpha_{i+1}}{\alpha_i}\sigma_i\right)\right]\boldsymbol{\varepsilon}_\theta(\mathbf{x}_i, i). \end{aligned} \tag{24}$$

By rearranging the BDIA (24), the inversion of BDIA is

$$\begin{aligned} \mathbf{x}_{i+1} =& \mathbf{x}_{i-1}/\gamma + (1-1/\gamma)\mathbf{x}_i + \Delta\left(i \to i+1 | \mathbf{x}_t\right) - (1/\gamma)\Delta\left(i \to i-1 | \mathbf{x}_i\right), \\ =& \frac{1}{\gamma}\mathbf{x}_{i-1} + \left(1 - \frac{1}{\gamma}\right)\mathbf{x}_i + \left[\left(\frac{\alpha_{i+1}}{\alpha_i} - 1\right)\mathbf{x}_i + \left(\sigma_{i+1} - \frac{\alpha_{i+1}}{\alpha_i}\sigma_i\right)\boldsymbol{\varepsilon}_\theta(x_i, i)\right] \\ &- \frac{1}{\gamma}\left[\left(\frac{\alpha_{i-1}}{\alpha_i} - 1\right)\mathbf{x}_i + \left(\sigma_{i-1} - \frac{\alpha_{i-1}}{\alpha_i}\sigma_i\right)\boldsymbol{\varepsilon}_\theta(\mathbf{x}_i, i)\right] \\ =& \frac{1}{\gamma}\mathbf{x}_{i-1} + \left(\frac{\alpha_{i+1}}{\alpha_i} - \frac{1}{\gamma}\frac{\alpha_{i-1}}{\alpha_i}\right)\mathbf{x}_i + \left[\left(\sigma_{i+1} - \frac{\alpha_{i+1}}{\alpha_i}\sigma_i\right) - \frac{1}{\gamma}\left(\sigma_{i-1} - \frac{\alpha_{i-1}}{\alpha_i}\sigma_i\right)\right]\boldsymbol{\varepsilon}_\theta(\mathbf{x}_i, i). \end{aligned} \tag{25}$$

A.3 Continuity Assumption and Other Mathematical Remarks

Continuity Assumption Much of our Local Truncation Error (LTE) analysis such as Proposition 1 and 4, is built on the Taylor expansion, which requires that the noise predictor satisfies the necessary continuity conditions. Therefore, we establish the following continuity assumption:

Assumption 2. *Denote $\boldsymbol{\mathcal{E}}_\theta(\bar{\sigma}_t) = \bar{\boldsymbol{\varepsilon}}_\theta(\bar{\mathbf{x}}(t), \bar{\sigma}_t)$, assume $\boldsymbol{\mathcal{E}}_\theta(\bar{\sigma}_t)$ is continuous w.r.t. $\bar{\sigma}_t$:*

$$\boldsymbol{\mathcal{E}}_\theta(\bar{\sigma}_t) \in C^\infty(\mathbb{R}, \mathbb{R}^n). \tag{26}$$

This assumption can be met by selecting a differentiable activation design in the noise predictor U-Net [49].

Variable of IVP Here, we further wish to clarify that the notation $\bar{\varepsilon}_\theta(\bar{\mathbf{x}}(t), \bar{\sigma}_t) \equiv \varepsilon_\theta(\mathbf{x}(t), t)$ presented in Section 3 is well-defined. This is because there exists a bijective relationship between $\bar{\sigma}_t$ and t, and $\bar{\mathbf{x}}(t)$ is simply a scaled version of $\mathbf{x}(t)$.

Singularity Issue In Assumption 1, we do not consider the singularity points at $t = 0$ and $t = 1$ because these points can lead to unusual performance of the noise predictor as discussed in [74]. In fact, our numerical method is minimally affected by these singularity points, thus making Assumption 1 reasonable.

A.4 Detailed Formulation of 3-step BELM

For 3-step BELM, we got five coefficients in the formulation:

$$\bar{\mathbf{x}}_{i-1} = a_{i,3}\bar{\mathbf{x}}_{i+2} + a_{i,2}\bar{\mathbf{x}}_{i+1} + a_{i,1}\bar{\mathbf{x}}_i + b_{i,2}h_{i+1}\bar{\varepsilon}_\theta(\bar{\mathbf{x}}_{i+1}, \bar{\sigma}_{i+1}) + b_{i,1}h_i\bar{\varepsilon}_\theta(\bar{\mathbf{x}}_i, \bar{\sigma}_i). \tag{27}$$

Follow the idea of Proposition 4, The local truncation error of the 3-step BELM diffusion sampler (27) τ_i can be accurate up to the fifth order of step sizes $\tau_i = \mathcal{O}\left((h_i + h_{i+1} + h_{i+2})^5\right)$ by setting coefficients as the following linear system

$$\begin{bmatrix} 1 & 1 & 1 & 0 & 0 \\ h_i & h_i + h_{i+1} & h_i + h_{i+1} + h_{i+2} & h_i & h_{i+1} \\ \frac{1}{2}h_i^2 & \frac{1}{2}(h_i + h_{i+1})^2 & \frac{1}{2}(h_i + h_{i+1} + h_{i+2})^2 & h_i^2 & h_{i+1}(h_i + h_{i+1}) \\ \frac{1}{6}h_i^3 & \frac{1}{6}(h_i + h_{i+1})^3 & \frac{1}{6}(h_i + h_{i+1} + h_{i+2})^3 & \frac{1}{2}h_i^3 & \frac{1}{2}h_{i+1}(h_i + h_{i+1})^2 \\ \frac{1}{24}h_i^4 & \frac{1}{24}(h_i + h_{i+1})^4 & \frac{1}{24}(h_i + h_{i+1} + h_{i+2})^4 & \frac{1}{6}h_i^4 & \frac{1}{6}h_{i+1}(h_i + h_{i+1})^3 \end{bmatrix} \begin{bmatrix} a_{i,1} \\ a_{i,2} \\ a_{i,3} \\ b_{i,1} \\ b_{i,2} \end{bmatrix} = \begin{bmatrix} 1 \\ 0 \\ 0 \\ 0 \\ 0 \end{bmatrix}. \tag{28}$$

There is no linear dependence between any two equations in (28). Through a calculation by hands or equation-solving tools like Matlab [27], the linear system above yields the unique solution provided below, which can be verified by readers.

$$\begin{bmatrix} a_{i,1} \\ a_{i,2} \\ a_{i,3} \\ b_{i,1} \\ b_{i,2} \end{bmatrix} = \begin{bmatrix} \frac{-((h_i+h_{i+1})^2(3h_i^2h_{i+1}+2h_i^2h_{i+2}+2h_ih_{i+1}^2+4h_ih_{i+1}h_{i+2}+2h_ih_{i+2}^2-h_{i+1}^3-2h_{i+1}^2h_{i+2}-h_{i+1}h_{i+2}^2))}{h_{i+1}^3(h_{i+1}+h_{i+2})^2} \\ \frac{(h_i^2(-h_i^2h_{i+1}+2h_i^2h_{i+2}-2h_ih_{i+1}^2+4h_ih_{i+1}h_{i+2}+2h_ih_{i+2}^2-h_{i+1}^3+2h_{i+1}^2h_{i+2}+3h_{i+1}h_{i+2}^2))}{h_{i+1}^3h_{i+2}^2} \\ \frac{h_i^2(h_i+h_{i+1})^2}{h_{i+2}^2(h_{i+1}+h_{i+2})^2} \\ \frac{-((h_i+h_{i+1})^2(h_i+h_{i+1}+h_{i+2}))}{h_{i+1}^2(h_{i+1}+h_{i+2})} \\ \frac{-(h_i^2(h_i+h_{i+1})(h_i+h_{i+1}+h_{i+2}))}{h_{i+1}^3h_{i+2}} \end{bmatrix}. \tag{29}$$

A.5 Detailed Formulation of k-step BELM

For general k-step BELM, we got $2k - 1$ coefficients in the formulation:

$$\bar{\mathbf{x}}_{i-1} = \sum_{j=1}^{k} a_{i,j} \cdot \bar{\mathbf{x}}_{i-1+j} + \sum_{j=1}^{k-1} b_{i,j} \cdot h_{i-1+j} \cdot \bar{\varepsilon}_\theta(\bar{\mathbf{x}}_{i-1+j}, \bar{\sigma}_{i-1+j}). \tag{30}$$

Following the derivation of 2-step case, we first applying the Taylor's expansion to $\bar{\mathbf{x}}_{i-1+j}$ and $\bar{\boldsymbol{\varepsilon}}_\theta(\bar{\mathbf{x}}_{i-1+j}, \bar{\sigma}_{i-1+j})$:

$$
\begin{aligned}
&\sum_{j=1}^{k} a_{i,j} \cdot \bar{\mathbf{x}}_{i-1+j} + \sum_{j=1}^{k-1} b_{i,j} \cdot h_{i-1+j} \cdot \bar{\boldsymbol{\varepsilon}}_\theta(\bar{\mathbf{x}}_{i-1+j}, \bar{\sigma}_{i-1+j}) \\
=&\sum_{j=1}^{k} a_{i,j} \left(\bar{\mathbf{x}}_{i-1} + \sum_{l=1}^{2k-2} \frac{1}{(l)!} \left(\sum_{m=0}^{j-1} h_{i+m} \right)^{l} \bar{\boldsymbol{\varepsilon}}_\theta^{(l-1)} \left(\bar{\mathbf{x}}(t_{i-1}), \bar{\sigma}_{i-1} \right) \right) \\
&+ \sum_{j=1}^{k-1} b_{i,j} h_{i-1+j} \left(\sum_{l=1}^{2k-2} \frac{1}{(l-1)!} \left(\sum_{m=0}^{j-1} h_{i+m} \right)^{l-1} \bar{\boldsymbol{\varepsilon}}_\theta^{(l-1)} \left(\bar{\mathbf{x}}(t_{i-1}), \bar{\sigma}_{i-1} \right) \right) \\
&+ \mathcal{O}\left(\left(\sum_{m=0}^{k-1} h_{i+m} \right)^{(2k-1)} \right) \qquad (31) \\
=&\sum_{j=1}^{k} a_{i,j} \bar{\mathbf{x}}_{i-1} + \sum_{l=1}^{2k-2} \left(\frac{1}{(l!)} \sum_{j=1}^{k} a_{i,j} \left(\sum_{m=1}^{j} h_{i+m-1} \right)^{l} \right) \bar{\boldsymbol{\varepsilon}}_\theta^{(l-1)} \left(\bar{\mathbf{x}}(t_{i-1}), \bar{\sigma}_{i-1} \right) \\
&+ \sum_{l=1}^{2k-2} \left(\frac{1}{((l-1)!)} \sum_{j=1}^{k-1} b_{i,j} h_{i+j-1} \left(\sum_{m=1}^{j} h_{i+m-1} \right)^{l-1} \right) \bar{\boldsymbol{\varepsilon}}_\theta^{(l-1)} \left(\bar{\mathbf{x}}(t_{i-1}), \bar{\sigma}_{i-1} \right) \\
&+ \mathcal{O}\left(\left(\sum_{m=0}^{k-1} h_{i+m} \right)^{(2k-1)} \right).
\end{aligned}
$$

Thus, the optimal coefficient can be computed by:

$$
\mathbf{A}_{(2k-1)\times(2k-1)} \begin{bmatrix} a_{i,1} \\ \vdots \\ a_{i,k} \\ b_{i,1} \\ \vdots \\ b_{i,k-1} \end{bmatrix}_{2k-1} = \begin{bmatrix} 1 \\ 0 \\ \vdots \\ 0 \end{bmatrix}_{2k-1}. \qquad (32)
$$

where $\mathbf{A} = [\mathbf{A}_1 \quad | \quad \mathbf{A}_2]$, and

$$
\mathbf{A}_1 = \begin{pmatrix}
1 & 1 & \cdots & 1 \\
h_i & h_i + h_{i+1} & \cdots & \sum_{j=0}^{k-1} h_{i+j} \\
\frac{1}{2} h_i^2 & \frac{1}{2}\left(h_i + h_{i+1}\right)^2 & \cdots & \frac{1}{2}\left(\sum_{j=0}^{k-1} h_{i+j}\right)^2 \\
\vdots & & \ddots & \vdots \\
\frac{1}{(2k-2)!} h_i^{2k-2} & \frac{1}{(2k-2)!}\left(h_i + h_{i+1}\right)^{2k-2} & \cdots & \frac{1}{(2k-2)!}\left(\sum_{j=0}^{k-1} h_{i+j}\right)^{2k-2}
\end{pmatrix}, \qquad (33)
$$

$$
\mathbf{A}_2 = \begin{pmatrix}
0 & 0 & \cdots & 0 \\
h_i & h_{i+1} & \cdots & h_{i+k-2} \\
h_i^2 & h_{i+1}\left(h_i + h_{i+1}\right) & \cdots & h_{i+k-2}\left(\sum_{j=0}^{k-2} h_{i+j}\right) \\
\frac{1}{2} h_i^3 & \frac{1}{2} h_{i+1}\left(h_i + h_{i+1}\right)^2 & \cdots & \frac{1}{2} h_{i+k-2}\left(\sum_{j=0}^{k-2} h_{i+j}\right)^2 \\
\vdots & & \ddots & \vdots \\
\frac{1}{(2k-3)!} h_i h_i^{2k-3} & \frac{1}{(2k-3)!} h_i \left(h_i + h_{i+1}\right)^{2k-3} & \cdots & \frac{1}{(2k-3)!} h_{i+k-2}\left(\sum_{j=0}^{k-2} h_{i+j}\right)^{2k-3}
\end{pmatrix}. \qquad (34)
$$

A.6 Definitions of Consistency

Consistency The consistency property refers to the ability of the method to accurately represent the IVP equation it's trying to solve. More specifically, a method is said to be consistent if, as the step size approaches zero, the difference between the numerical method and the exact differential equation also approaches zero.

Definition 4. *The LM method* (12) *is* ***consistent*** *if for every function* $y \in C^1[t_0, t_0 + T]$

$$\lim_{h \to 0} \sum_{i=k}^{N-1} \|\tau_i\| = 0. \tag{35}$$

A.7 BDIA as a Sub-Optimal Special Case of BELM

the updating rule of BDIA write:

$$\mathbf{x}_{i-1} = \gamma \mathbf{x}_{i+1} + \left(\frac{\alpha_{i-1}}{\alpha_i} - \gamma \frac{\alpha_{i+1}}{\alpha_i} \right) \mathbf{x}_i + \left[\sigma_{i-1} - \frac{\alpha_{i-1}}{\alpha_i} \sigma_i - \gamma \left(\sigma_{i+1} - \frac{\alpha_{i+1}}{\alpha_i} \sigma_i \right) \right] \boldsymbol{\varepsilon}_\theta(\mathbf{x}_i, i). \tag{36}$$

With the same alpha, scaled sigma and stepsize schedule as the BELM, the BDIA update (36) have an equivalent **bidirectional explicit** linear multi-step form with an easy rearrangement,

$$\bar{\mathbf{x}}_{i-1} = a_{i,2} \cdot \bar{\mathbf{x}}_{i+1} + a_{i,1} \cdot \bar{\mathbf{x}}_i + b_{i,1} \cdot h_i \cdot \bar{\boldsymbol{\varepsilon}}_\theta(\bar{\mathbf{x}}_i, \bar{\sigma}_i), \tag{37}$$

where

$$a_{i,2} = \gamma \frac{\alpha_{i+1}}{\alpha_{i-1}}, \qquad a_{i,1} = 1 - \gamma \frac{\alpha_{i+1}}{\alpha_{i-1}}, \qquad b_{i,1} = -1 - \gamma \frac{\alpha_{i+1}}{\alpha_{i-1}} \frac{h_{i+1}}{h_i}. \tag{38}$$

Thus we find that BDIA is indeed a special case of our BELM framework.

A.8 EDICT as a Sub-Optimal Special Case of BELM

In this section, we will demonstrate that a sequence of $\{\mathbf{x}_i\}$, $\{\mathbf{y}_i\}$, $\{\mathbf{y}_i^{inter}\}$, and $\{\mathbf{x}_i^{inter}\}$, where $i \in [N \dots 1]$, generated by EDICT (9), indeed corresponds to a sequence of $\mathbf{z}_j$, where $j \in [4N \dots 1]$, produced by a special BELM. The EDICT updates as follows:

$$\begin{cases} \mathbf{x}_i^{inter} = \frac{\alpha_{i-1}}{\alpha_i} \mathbf{x}_i + \left(\sigma_{i-1} - \frac{\alpha_{i-1}}{\alpha_i} \sigma_i \right) \boldsymbol{\varepsilon}_\theta(\mathbf{y}_i, i), \\ \mathbf{y}_i^{inter} = \frac{\alpha_{i-1}}{\alpha_i} \mathbf{y}_i + \left(\sigma_{i-1} - \frac{\alpha_{i-1}}{\alpha_i} \sigma_i \right) \boldsymbol{\varepsilon}_\theta(\mathbf{x}(t)^{inter}, i), \\ \mathbf{x}_{i-1} = p\mathbf{x}_i^{inter} + (1-p)\mathbf{y}_i^{inter}, \\ \mathbf{y}_{i-1} = p\mathbf{y}_i^{inter} + (1-p)\mathbf{x}_{i-1}. \end{cases} \tag{39}$$

transfer $\mathbf{x}_i$ to $\mathbf{z}_{4l}$, $\mathbf{y}_i$ to $\mathbf{z}_{4l-1}$, $\mathbf{x}_i^{inter}$ to $\mathbf{z}_{4l-2}$ and $\mathbf{y}_i^{inter}$ to $\mathbf{z}_{4l-3}$,

$$\begin{cases} \mathbf{z}_{4l-2} = \frac{\alpha_{i-1}}{\alpha_i} \mathbf{z}_{4l} + \left(\sigma_{i-1} - \frac{\alpha_{i-1}}{\alpha_i} \sigma_i \right) \boldsymbol{\varepsilon}_\theta(\mathbf{z}_{4l-1}, i), \\ \mathbf{z}_{4l-3} = \frac{\alpha_{i-1}}{\alpha_i} \mathbf{z}_{4l-1} + \left(\sigma_{i-1} - \frac{\alpha_{i-1}}{\alpha_i} \sigma_i \right) \boldsymbol{\varepsilon}_\theta(\mathbf{z}_{4l-2}, i), \\ \mathbf{z}_{4l-4} = p\mathbf{z}_{4l-2} + (1-p)\mathbf{z}_{4l-3}, \\ \mathbf{z}_{4l-5} = p\mathbf{z}_{4l-3} + (1-p)\mathbf{z}_{4l-4}. \end{cases} \tag{40}$$

We set alpha schedule to be

$$\alpha_{4l} = \alpha_i, \quad \alpha_{4l-1} = \alpha_i, \quad \alpha_{4l-2} = \sqrt{\alpha_i \alpha_{i-1}}, \quad \alpha_{4l-3} = \alpha_{i-1}. \tag{41}$$

Then we set sigma schedule to be

$$\sigma_{4l} = \sigma_i, \quad \sigma_{4l-1} = \sigma_i, \quad \sigma_{4l-2} = \frac{1}{2} \left(\sigma_i \frac{\sqrt{\alpha_{i-1}}}{\sqrt{\alpha_i}} + \sigma_{i-1} \frac{\sqrt{\alpha_i}}{\sqrt{\alpha_{i-1}}} \right), \quad \sigma_{4l-3} = \sigma_{i-1}. \tag{42}$$

Thus the scaled sigma writes

$$\bar{\sigma}_{4l} = \bar{\sigma}_{4l-1} = \frac{\sigma_i}{\alpha_i}, \quad \bar{\sigma}_{4l-2} = \frac{\sigma_i}{\alpha_i} + \frac{\sigma_{i-1}}{\alpha_{i-1}}, \quad \bar{\sigma}_{4l-3} = \frac{\sigma_{i-1}}{\alpha_{i-1}}. \tag{43}$$

And the stepsize schedule will be

$$h_{4l} = 0, \quad h_{4l-1} = \frac{1}{2}\left(\frac{\sigma_i}{\alpha_i} - \frac{\sigma_{i-1}}{\alpha_{i-1}}\right), \quad h_{4l-2} = \frac{1}{2}\left(\frac{\sigma_i}{\alpha_i} - \frac{\sigma_{i-1}}{\alpha_{i-1}}\right), \quad h_{4l-3} = 0. \tag{44}$$

With easy substitution, the EDICT update (40) have an equivalent **bidirectional explicit** linear multi-step form:

$$\bar{\mathbf{z}}_{j-1} = a_{j,2} \cdot \bar{\mathbf{z}}_{j+1} + a_{j,1} \cdot \bar{\mathbf{z}}_j + b_{j,1} \cdot h_j \cdot \bar{\varepsilon}_\theta(\bar{\mathbf{z}}_j, \bar{\sigma}_j) \tag{45}$$

where the coefficients take the following piece-wise function form:

$$a_{j,2} = \begin{cases} p\frac{\sqrt{\alpha_{i+1}}}{\sqrt{\alpha_i}}, j = 4l \\ p, j = 4l-1 \\ \frac{\sqrt{\alpha_{i-1}}}{\sqrt{\alpha_i}}, j = 4l-2 \\ 1, j = 4l-3 \end{cases} \quad a_{j,1} = \begin{cases} 1-p, j = 4l \\ 1-p, j = 4l-1 \\ 0, j = 4l-2 \\ 0, j = 4l-3 \end{cases} \quad b_{j,1} = \begin{cases} 0, j = 4l \\ 0, j = 4l-1 \\ -2\frac{\sqrt{\alpha_{i-1}}}{\sqrt{\alpha_i}}, j = 4l-2 \\ -2, j = 4l-3 \end{cases} \tag{46}$$

Despite the formulation of (9) being subject to cyclic variations, the variable $a_{j,2}$ consistently remains non-zero, thereby satisfying the conditions of the BELM framework. Consequently, EDICT can indeed be considered a special case within our BELM framework.

A.9 Order of Accuracy

In this section, we further explore the order of accuracy of DDIM, EDICT, BDIA, and our proposed O-BELM. Our findings indicate that O-BELM achieves the superior order of accuracy among these methods. Intuitively, the order of accuracy provides insight into which functional class of the IVP can be accurately approximated by a given method.

Definition 5. *The method* (14) *is said to have* ***order of accuracy p*** *if p is the largest positive integer such that there exist constants K and h^* such that for all i,*

$$\|\tau_i\| \leq K h^{p+1}, \quad for \quad 0 < h < h^*. \tag{47}$$

Proposition 6. *The BELM diffusion sampler* (15) *is with* ***second-order accuracy****; The DDIM diffusion sampler* (7) *is with* ***first-order accuracy****; The EDICT diffusion sampler* (9) *is with* ***zero-order accuracy****; The BDIA diffusion sampler* (10) *is with* ***first-order accuracy****.*

Proof. This proposition can be directly inferred from the Definition 5, in conjunction with Proposition 1 and 4. □

Remark 2. *Though the order of accuracy of BDIA is the same as DDIM to be 1, its step size in local error of BDIA is about twice that of DDIM. This theoretical result confirms the experimental observation that the sampling quality of BDIA sometimes is inferior to that of DDIM.*

A.10 Further Theoretical Properties of DDIM

We have also conducted an analysis of global stability and convergence for DDIM. It is apparent that the success of DDIM fundamentally stems from its nice theoretical property. Our O-BELM preserves these excellent theoretical properties of DDIM and maintains high-quality sampling performance.

Proposition 7. *The DDIM diffusion sampler* (7) *is (a)* ***zero-stable*** *and (b)* ***globally convergent****.*

A.11 Pseudocode for O-BELM Sampling Process

To more effectively elucidate the implementation of O-BELM, we provide the pseudocode for O-BELM in Algorithm 1. Upon examination, it is apparent that the implementation of O-BELM requires little modifications compared to DDIM, thus facilitating its easy portability to pretrained models.

Algorithm 1 O-BELM sampling process

```
Input: pretrained noise predictor ε_θ, number of timesteps N, noise schedule {α_t} and {σ_t},
    x_list = [].
Sample x_N ~ N(0, σ_{t_N} I).
x_list.append(x_N)
for i = N, N−1, ..., 1 do
    if i < N then
        Calculate h_i, a_{i,1}, a_{i,2} and b_{i,1} according to (53).
        x_{i−1} = a_{i,1} x_list[-1] + a_{i,2} x_list[-2] + b_{i,1} h_i ε_θ(x_list[-1], i)
    else
        x_{i−1} = (α_{i−1}/α_i) x_list[-1] + (σ_{i−1} − (α_{i−1}/α_i) σ_i) ε_θ(x_list[-1], i).
    end if
    x_list.append(x_{i−1})
end for
Output: x_list
```

B Proofs

B.1 Proof of Proposition 2

Proof. We demonstrate the exact inversion property of BELM (14) by initially establishing that its local reconstruction error is zero. Assuming that we have already obtained $\{\bar{\mathbf{x}}_{i-1+j}\}_{j=1}^{k}$, we compute $\bar{\mathbf{x}}_{i-1}$ in accordance with (14), as follows:

$$\bar{\mathbf{x}}_{i-1} = \sum_{j=1}^{k} a_{i,j} \cdot \bar{\mathbf{x}}_{i-1+j} + \sum_{j=1}^{k-1} b_{i,j} \cdot h_{i-1+j} \cdot \bar{\boldsymbol{\varepsilon}}_\theta(\bar{\mathbf{x}}_{i-1+j}, \bar{\sigma}_{i-1+j}), \tag{48}$$

and we will use $\{\bar{\mathbf{x}}_{i-1+j}\}_{j=0}^{k-1}$ to reconstruct $\tilde{\bar{\mathbf{x}}}_{i-1+k}$ according to (13), as follows:

$$\tilde{\bar{\mathbf{x}}}_{i-1+k} = \frac{1}{a_{i,k}} \cdot \bar{\mathbf{x}}_{i-1} - \sum_{j=1}^{k-1} \frac{a_{i,j}}{a_{i,k}} \cdot \bar{\mathbf{x}}_{i-1+j} + \sum_{j=0}^{k} \frac{b_{i,j}}{a_{i,k}} \cdot h_{i-1+j} \cdot \bar{\boldsymbol{\varepsilon}}_\theta(\bar{\mathbf{x}}_{i-1+j}, \bar{\sigma}_{i-1+j}). \tag{49}$$

The local reconstruction error, defined as the difference between $\tilde{\bar{\mathbf{x}}}_{i-1+k}$ and $\bar{\mathbf{x}}_{i-1+k}$, can be calculated and is found to be zero. Furthermore, global exact inversion can be inferred from local exact inversion through the application of Mathematical Induction (MI). □

B.2 Proof of Proposition 3

Proof. The Local Truncation Error (LTE) of the BELM diffusion sampler (15) can be computed by substituting $\bar{\mathbf{x}}(t_i)$, $\bar{\mathbf{x}}(t_{i+1})$, and $\bar{\varepsilon}_\theta(\bar{\mathbf{x}}(t_i), \bar{\sigma}_i)$ in(16) with their corresponding Taylor expansions at

$\bar{\sigma}_{i-1}$ as follows:

$$\begin{aligned}
\tau_i =&\bar{\mathbf{x}}(t_{i-1}) - a_{i,1} \cdot \bar{\mathbf{x}}(t_i) - a_{i,2} \cdot \bar{\mathbf{x}}(t_{i+1}) - b_{i,1} \cdot h_i \cdot \bar{\boldsymbol{\varepsilon}}_\theta(\bar{\mathbf{x}}(t_i), \bar{\sigma}_i) \\
=&\bar{\mathbf{x}}(t_{i-1}) - a_{i,1} \left[\bar{\mathbf{x}}(t_{i-1}) + \frac{\bar{\boldsymbol{\varepsilon}}_\theta\left(\bar{\mathbf{x}}(t_{i-1}), \bar{\sigma}_{i-1}\right)}{1!}(h_i)\right. \\
&\left. + \frac{\nabla_{\bar{\sigma}_{i-1}} \bar{\boldsymbol{\varepsilon}}_\theta\left(\bar{\mathbf{x}}(t_{i-1}), \bar{\sigma}_{i-1}\right)}{2!}(h_i)^2 + \mathcal{O}\left({h_i}^3\right)\right] \\
&- a_{i,2} \left[\bar{\mathbf{x}}(t_{i-1}) + \frac{\bar{\boldsymbol{\varepsilon}}_\theta\left(\bar{\mathbf{x}}(t_{i-1}), \bar{\sigma}_{i-1}\right)}{1!}(h_i + h_{i+1}) + \right. \\
&\left. \frac{\nabla_{\bar{\sigma}_{i-1}} \bar{\boldsymbol{\varepsilon}}_\theta\left(\bar{\mathbf{x}}(t_{i-1}), \bar{\sigma}_{i-1}\right)}{2!}(h_i + h_{i+1})^2 + \mathcal{O}\left((h_i + h_{i+1})^3\right)\right] \\
&- b_{i,1} \cdot h_i \left[\bar{\boldsymbol{\varepsilon}}_\theta\left(\bar{\mathbf{x}}(t_{i-1}), \bar{\sigma}_{i-1}\right) + \frac{\nabla_{\bar{\sigma}_{i-1}} \bar{\boldsymbol{\varepsilon}}_\theta\left(\bar{\mathbf{x}}(t_{i-1}), \bar{\sigma}_{i-1}\right)}{1!}(h_i) + \mathcal{O}\left({h_i}^2\right)\right] \\
=& \left(1 - a_{i,1} - a_{i,2}\right) \bar{\mathbf{x}}(t_{i-1}) \\
&+ \left[-a_{i,1} h_i - a_{i,2}\left(h_i + h_{i+1}\right) - b_{i,1} \cdot h_i\right] \cdot \bar{\boldsymbol{\varepsilon}}_\theta\left(\bar{\mathbf{x}}(t_{i-1}), \bar{\sigma}_{i-1}\right) \\
&+ \left[-\frac{a_{i,1}}{2} \cdot h_i^2 - \frac{a_{i,2}}{2}(h_i + h_{i+1})^2 - b_{i,1} \cdot h_i^2\right] \cdot \nabla_{\bar{\sigma}_{i-1}} \bar{\boldsymbol{\varepsilon}}_\theta\left(\bar{\mathbf{x}}(t_{i-1}), \bar{\sigma}_{i-1}\right) \\
&+ \mathcal{O}\left((h_i + h_{i+1})^3\right).
\end{aligned} \tag{50}$$

□

B.3 Proof of Proposition 4

Proof. In the (17) of Proposition 3, we have three degrees of freedom: $a_{i,1}$, $a_{i,2}$, and $b_{i,1}$ in the LTE of BELM (15). Therefore, the highest order that τ_i can achieve is three, under the condition that:

$$\begin{cases} 1 - a_{i,1} - a_{i,2} = 0, \\ -a_{i,1} h_i - a_{i,2}\left(h_i + h_{i+1}\right) - b_{i,1} \cdot h_i = 0, \\ -\frac{a_{i,1}}{2} \cdot h_i^2 - \frac{a_{i,2}}{2}(h_i + h_{i+1})^2 - b_{i,1} \cdot h_i^2 = 0. \end{cases} \tag{51}$$

whose matrix form writes

$$\begin{bmatrix} 1 & 1 & 0 \\ h_i & (h_i + h_{i+1}) & h_i \\ \frac{1}{2} h_i^2 & \frac{1}{2}(h_i + h_{i+1})^2 & h_i^2 \end{bmatrix} \begin{bmatrix} a_{i,1} \\ a_{i,2} \\ b_{i,1} \end{bmatrix} = \begin{bmatrix} 1 \\ 0 \\ 0 \end{bmatrix}. \tag{52}$$

There is no linear dependence between any two equations in (51). Through a straightforward calculation, the linear system above yields the unique solution provided below, which can be verified by readers.

$$a_{i,1} = \frac{h_{i+1}^2 - h_i^2}{h_{i+1}^2}, \quad a_{i,2} = \frac{h_i^2}{h_{i+1}^2}, \quad b_{i,1} = -\frac{h_i + h_{i+1}}{h_{i+1}}. \tag{53}$$

□

B.4 Proof of Corollary 1

B.4.1 LTE of DDIM

Proposition 8. *The LTE* $\mathbf{e}_i$ *of DDIM sampler* (7) *is* $\mathcal{O}\left(\alpha_{i-1} {h_i}^2\right)$.

Proof. By applying the Taylor expansion and substitute into the DDIM formulation (7), we can calculate the local error of DDIM on $\mathbf{x}_i$ as following.

$$
\begin{aligned}
\mathbf{e}_i =&\mathbf{x}(t_{i-1}) - \frac{\alpha_{i-1}}{\alpha_i}\mathbf{x}(t_i) - \left(\sigma_{i-1} - \frac{\alpha_{i-1}}{\alpha_i}\sigma_i\right)\bar{\boldsymbol{\varepsilon}}_\theta\left(\bar{\mathbf{x}}(t_i), \bar{\sigma}_i\right) \\
=&\mathbf{x}(t_{i-1}) - \frac{\alpha_{i-1}}{\alpha_i}\alpha_i\left(\frac{\mathbf{x}(t_{i-1})}{\alpha_{i-1}} + \frac{\bar{\boldsymbol{\varepsilon}}_\theta\left(\bar{\mathbf{x}}(t_{i-1}), \bar{\sigma}_{i-1}\right)}{1!}(h_i) + \mathcal{O}\left({h_i}^2\right)\right) \\
&-(-h_i)\,\alpha_{i-1}\left(\bar{\boldsymbol{\varepsilon}}_\theta\left(\bar{\mathbf{x}}(t_{i-1}), \bar{\sigma}_{i-1}\right) + \mathcal{O}\left(h_i\right)\right) \\
=&\mathcal{O}\left(\alpha_{i-1}{h_i}^2\right).
\end{aligned} \tag{54}
$$

□

B.4.2 LTE of BDIA

Proposition 9. *The LTE $\mathbf{e}_i$ of BDIA sampler* (10) *is $\mathcal{O}\left(\alpha_{i-1}(h_i + h_{i+1})^2\right)$ for any fixed $\gamma \in [0, 1]$.*

Proof. By applying the Taylor expansion and substitute into the BDIA formulation (10), we can calculate the local error of BDIA on $\mathbf{x}_i$ as following.

$$
\begin{aligned}
\mathbf{e}_i =&\mathbf{x}(t_{i-1}) - \gamma\mathbf{x}(t_{i+1}) - \left(\frac{\alpha_{i-1}}{\alpha_i} - \gamma\frac{\alpha_{i+1}}{\alpha_i}\right)\mathbf{x}(t_i) \\
&-\left[\sigma_{i-1} - \frac{\alpha_{i-1}}{\alpha_i}\sigma_i - \gamma\left(\sigma_{i+1} - \frac{\alpha_{i+1}}{\alpha_i}\sigma_i\right)\right]\bar{\boldsymbol{\varepsilon}}_\theta\left(\bar{\mathbf{x}}(t_i), \bar{\sigma}_i\right) \\
=&\mathbf{x}(t_{i-1}) - \gamma\alpha_{i+1}\left[\frac{\mathbf{x}(t_{i-1})}{\alpha_{i-1}} + \frac{\bar{\boldsymbol{\varepsilon}}_\theta\left(\bar{\mathbf{x}}(t_{i-1}), \bar{\sigma}_{i-1}\right)}{1!}(h_i + h_{i+1}) + \right. \\
&\left.\frac{\nabla_{\bar{\sigma}_{i-1}}\bar{\boldsymbol{\varepsilon}}_\theta\left(\bar{\mathbf{x}}(t_{i-1}), \bar{\sigma}_{i-1}\right)}{2!}(h_i + h_{i+1})^2 + \mathcal{O}\left((h_i + h_{i+1})^3\right)\right] \\
&-\left(\frac{\alpha_{i-1}}{\alpha_i} - \gamma\frac{\alpha_{i+1}}{\alpha_i}\right)\alpha_i\left[\frac{\mathbf{x}(t_{i-1})}{\alpha_{i-1}} + \frac{\bar{\boldsymbol{\varepsilon}}_\theta\left(\bar{\mathbf{x}}(t_{i-1}), \bar{\sigma}_{i-1}\right)}{1!}(h_i)\right. \\
&\left.+\frac{\nabla_{\bar{\sigma}_{i-1}}\bar{\boldsymbol{\varepsilon}}_\theta\left(\bar{\mathbf{x}}(t_{i-1}), \bar{\sigma}_{i-1}\right)}{2!}(h_i)^2 + \mathcal{O}\left({h_i}^3\right)\right] \\
&-\left[\sigma_{i-1} - \frac{\alpha_{i-1}}{\alpha_i}\sigma_i - \gamma\left(\sigma_{i+1} - \frac{\alpha_{i+1}}{\alpha_i}\sigma_i\right)\right]\left[\bar{\boldsymbol{\varepsilon}}_\theta\left(\bar{\mathbf{x}}(t_{i-1}), \bar{\sigma}_{i-1}\right)\right. \\
&\left.+\frac{\nabla_{\bar{\sigma}_{i-1}}\bar{\boldsymbol{\varepsilon}}_\theta\left(\bar{\mathbf{x}}(t_{i-1}), \bar{\sigma}_{i-1}\right)}{1!}(h_i) + \mathcal{O}\left({h_i}^2\right)\right] \\
=&\left(-\frac{\gamma}{2}\alpha_{i+1}h_{i+1}^2 + \frac{3}{2}\alpha_{i-1}h_i^2\right)\nabla_{\bar{\sigma}_{i-1}}\bar{\boldsymbol{\varepsilon}}_\theta\left(\bar{\mathbf{x}}(t_{i-1}), \bar{\sigma}_{i-1}\right) + \mathcal{O}\left({h_i}^3\right).
\end{aligned} \tag{55}
$$

For a fixed γ, the term $\bar{\varepsilon}_\theta\left(\bar{\mathbf{x}}(t_{i-1}), \bar{\sigma}_{i-1}\right)$ cannot be eliminated for every i. This is due to the fact that the second-order term $-\frac{\gamma}{2}\alpha_{i+1}h_{i+1}^2 + \frac{3}{2}\alpha_{i-1}h_i^2$ is dynamic with respect to i. Consequently, the second-order local error will persist in the BDIA. □

B.4.3 LTE of EDICT

Proposition 10. *The LTE $\mathbf{e}_i$ of EDICT sampler* (9) *is $\mathcal{O}\left(\sqrt{\alpha_{i-1}}h_i\right)$ for any constant $p \in (0, 1)$.*

To prove the Proposition 10, we need first establish an order estimate lemma:

Lemma 1. *The term $\sqrt{\alpha_i} - \sqrt{\alpha_{i-1}}$ have order $\mathcal{O}\left(h_i\right)$*

Proof. Recall that we define h_i to be $\bar{\sigma}_i - \bar{\sigma}_{i-1}$. In order to figure out the relation of $\sqrt{\alpha_i} - \sqrt{\alpha_{i-1}}$ w.r.t. $\bar{\sigma}_i - \bar{\sigma}_{i-1}$, we first use $\bar{\sigma}$ to represent $\sqrt{\alpha}$:

$$\begin{aligned}\bar{\sigma} &= \frac{\sqrt{1-\alpha^2}}{\alpha} \\ \bar{\sigma}^2 &= \frac{1-\alpha^2}{\alpha^2} \\ (\bar{\sigma}^2+1)\alpha^2 &= 1 \\ \alpha &= \sqrt{\frac{1}{\bar{\sigma}^2+1}} \\ \sqrt{\alpha} &= \left(\bar{\sigma}^2+1\right)^{-\frac{1}{4}}.\end{aligned} \tag{56}$$

We then discover that $\mathrm{d}\sqrt{\alpha} = -\frac{1}{2}\left(\bar{\sigma}^2+1\right)^{-\frac{5}{4}}\bar{\sigma}\mathrm{d}\bar{\sigma} \sim C\mathrm{d}\bar{\sigma}$. This implies that $\sqrt{\alpha_i} - \sqrt{\alpha_{i-1}}$ and $\bar{\sigma}_i - \bar{\sigma}_{i-1}$ are of the same order, which is h_i. □

Now we can start to prove Proposition 10:

Proof. Since larger errors can absorb smaller ones, the $4l$ and $4l-2$ terms in (46) introduce errors in the zeroth order of the Taylor expansion. This is where the main error occurs. Both of these updates introduce an error of $\frac{\sqrt{\alpha_i}-\sqrt{\alpha_{i-1}}}{\sqrt{\alpha_i}}$ on $\bar{\mathbf{x}}_i$, which means that the error on $\mathbf{x}_i$ is $\sqrt{\alpha_i}\left(\sqrt{\alpha_i} - \sqrt{\alpha_{i-1}}\right)$. Therefore, according to Lemma 1, the error e_i is of the order $\mathcal{O}\left(\sqrt{\alpha_i}h_i\right)$. □

Remark 3. *Please note that we have only established an error bound for EDICT based on the perspective of the linear multiplication method. There may be a tighter bound of EDICT on constants when viewed from the perspective of an interactive mixing system.*

B.5 Proof of Proposition 5(a) and Proposition 7(a)

Assumption 3. *$\bar{\sigma}_i$ is strictly concave w.r.t. i.*

$\bar{\sigma}_i$ w.r.t i is a composition of $\bar{\sigma}_i$ w.r.t α_i and α_i w.r.t. i. $\bar{\sigma}_i = \frac{\sqrt{1-\alpha_i^2}}{\alpha_i}$ which is non-increasing and strictly convex. Thus Assumption 3 can be achieved by choosing schedule of α_i to be strictly convex w.r.t. i.

Lemma 2. *There exist a real constant C which is independent of α_t and σ_t, such that for every i, we have $|a_{i,1}| \le C$, $|a_{i,2}| \le C$ and $|b_{i,1}| \le C$ in* (15).

We will use an variable-stepsize-variable-formula analogy of the root condition of Dahlquist [9] to prove the zero-stability of (15).

Theorem 1. *[8, (3.10)] Define the root matrix of a LM 12 at step i to be $\mathbf{R}_i$,*

$$\mathbf{R}_i = \begin{pmatrix} a_{i,1} & \cdots & \cdots & a_{i,k} \\ 1 & 0 & & 0 \\ \vdots & \ddots & \ddots & \vdots \\ 0 & & 1 & 0 \end{pmatrix}. \tag{57}$$

If all coefficients can be bounded and there exists a regular matrix $\mathbf{H}$ such that for all i

$$\left\|\mathbf{H}^{-1}\mathbf{R}_i\mathbf{H}\right\|_1 \le 1, \tag{58}$$

then the LM 12 is zero-stable.

Finally, we start to give the proof of Proposition 5(a) under the Assumption 3.

Proposition 11. *The O-BELM diffusion sampler* (18) *is zero-stable.*

Proof. the root matrix of (15) writes

$$\mathbf{R}_i = \begin{bmatrix} \frac{h_{i+1}^2 - h_i^2}{h_{i+1}^2} & \frac{h_i^2}{h_{i+1}^2} \\ 1 & 0 \end{bmatrix}. \tag{59}$$

The Assumption 3 can reach to $\bar{\sigma}_{i+1} + \bar{\sigma}_{i-1} < 2\bar{\sigma}_i$, thus $h_{i+1} < h_i < 0$. Then we denote $\eta = \max_i \frac{h_i^2}{h_{i+1}^2} < 1$, by setting $\mathbf{H}$ as following

$$\mathbf{H} = \begin{bmatrix} 1 & \frac{2}{1-\eta} \\ 0 & \frac{2}{1-\eta} \end{bmatrix}, \tag{60}$$

then we can calculate that

$$\begin{aligned} \left\|\mathbf{H}^{-1}\mathbf{R}_i\mathbf{H}\right\|_1 &= \left\| \begin{bmatrix} 1 & \frac{2}{1-\eta} \\ 0 & \frac{2}{1-\eta} \end{bmatrix}^{-1} \begin{bmatrix} \frac{h_{i+1}^2 - h_i^2}{h_{i+1}^2} & \frac{h_i^2}{h_{i+1}^2} \\ 1 & 0 \end{bmatrix} \begin{bmatrix} 1 & \frac{2}{1-\eta} \\ 0 & \frac{2}{1-\eta} \end{bmatrix} \right\|_1 \\ &= \max\left(\frac{|\frac{\eta}{2} - \frac{1}{2}||h_{i+1}|^2 + |h_i|^2}{|h_{i+1}|^2}, \frac{2|\frac{\eta}{2} - \frac{1}{2}|}{|\eta - 1|} \right), \end{aligned} \tag{61}$$

where we can compute that

$$\begin{aligned} &\frac{|\frac{\eta}{2} - \frac{1}{2}||h_{i+1}|^2 + |h_i|^2}{|h_{i+1}|^2} \\ &= \left|\frac{\eta}{2} - \frac{1}{2}\right| + \frac{h_i^2}{h_{i+1}^2} \\ &= \frac{1}{2} - \frac{\eta}{2} + \frac{h_i^2}{h_{i+1}^2} \\ &< \frac{1}{2} - \frac{1}{2}\frac{h_i^2}{h_{i+1}^2} + \frac{h_i^2}{h_{i+1}^2} \\ &= \frac{1}{2}\frac{h_i^2 + h_{i+1}^2}{h_{i+1}^2} \\ &< 1, \end{aligned} \tag{62}$$

and obviously

$$\frac{2|\frac{\eta}{2} - \frac{1}{2}|}{|\eta - 1|} = 1. \tag{63}$$

Consequently, we have the conclusion that for all i, the requirement of $\left\|\mathbf{H}^{-1}\mathbf{R}_i\mathbf{H}\right\|_1 \leq 1$ is satisfied. Thus due to Theorem 1, The BELM diffusion sampler (15) is zero-stable. □

Remark 4. *Here, we present a very strong proof of Proposition 11 under Assumption 3, demonstrating that the iterative mapping of BELM constitutes a contraction mapping at each step i. However, it is important to note that in practical applications, even if Assumption 3 is not met at some step i, resulting in $\mathbf{R}_i$ not being contractive sometimes, global stability may still be achieved.*

The proof for Proposition 7(a) writes:

Proof. As DDIM can be seen as an explicit Euler method to the diffusion IVP, following the same reasoning of B.5, the root matrix of DDIM is $\mathbf{R}_i = \mathbf{I}$. Obviously, DDIM is zero-stable. □

B.6 Proof of Proposition 5(b) and Proposition 7(b)

To analyse the global convergence property of a method, we first need to analyse the consistency property of a method. Please look up the definition of consistency in Appendix A.6. We first establish the consistency of DDIM and BELM by the following theorem.

Theorem 2. *[8, (2.5.1)] If a method have an order of accuracy 1 and all its coefficients is bounded by constant, then it is consistent.*

Lemma 3. *The BELM diffusion sampler* (15) *is consistent.*

Proof. This lemma is a direct result of Lemma 2, Proposition 6 and Theorem 2. □

Lemma 4. *The DDIM diffusion sampler* (7) *is consistent.*

Proof. In common choice of noise schedule, $\frac{\alpha_{i-1}}{\alpha_i}$ and $\sigma_{i-1} - \frac{\alpha_{i-1}}{\alpha_i}\sigma_i$ is bounded. Thus this lemma is a direct result of Theorem 2. □

After we establish the consistency of DDIM and BELM, we can prove their global convergence by a famous sufficiency of conditions for convergence.

Theorem 3. *[3, p.342 (Theorem 406D)] A linear multistep method is convergent if it is consistent and zero-stable.*

With the help of Theorem 3, we can reach to Proposition 7(b) by Lemma 4 and Proposition 7(a); and reach to Proposition 5(b) by Lemma 3 and Proposition 11.

C Experiments Details and Extra Results

In these image tasks, we only apply our 2-step O-BELM, as it has been demonstrated that higher-order numerical methods can lead to strong oscillations in stiff spaces such as images [58, p.343]. However, the application of higher-order O-BELM in other domains of Diffusion Models (DMs) continues to hold promise.

For the sake of open accessibility, the dataset used in this paper is publicly available on the internet. We have included codes, accompanied by corresponding instructions, in the supplementary materials and plan to make them accessible on GitHub. However, our Stable Diffusion-related code is intricately interwoven with our proprietary business code, and we are in the process of decoupling the codebase. As soon as this task is completed, we will make the codes available on GitHub.

C.1 Image Reconstruction

Figure 4 presents the reconstruction results from several example images under 50 steps. It is evident that DDIM reconstructs images with non-negligible distortions compared to the original images, as marked by the red rectangle in Figure 4. Our findings suggest that the exact inversion samplers (EDICT, BDIA, and O-BELM) indeed achieve exact inversion at the latent level, thereby achieving the lower bound of the reconstruction error of AE in latent diffusion models. Although the encoding and decoding processes of AE introduce some reconstruction error, these errors do not result in any detectable inconsistencies in the image as perceived by the human eye. It's also important to note that exact inversion requires the storage of two intermediates for precise reconstruction. This is feasible in downstream tasks such as image editing.

We have also conducted an additional experiment to assess the reconstruction error in the latent space of O-BELM and other baseline methods as shown in Figure 5.

Table 5: Comparison of different samplers on MSE reconstruction loss on latent space on COCO-14.

	MSE loss of reconstruction on latents			
	DDIM	EDICT	BDIA	**O-BELM**
10 steps	0.414	0.000	0.000	0.000
20 steps	0.243	0.000	0.000	0.000
50 steps	0.063	0.000	0.000	0.000
100 steps	0.041	0.000	0.000	0.000

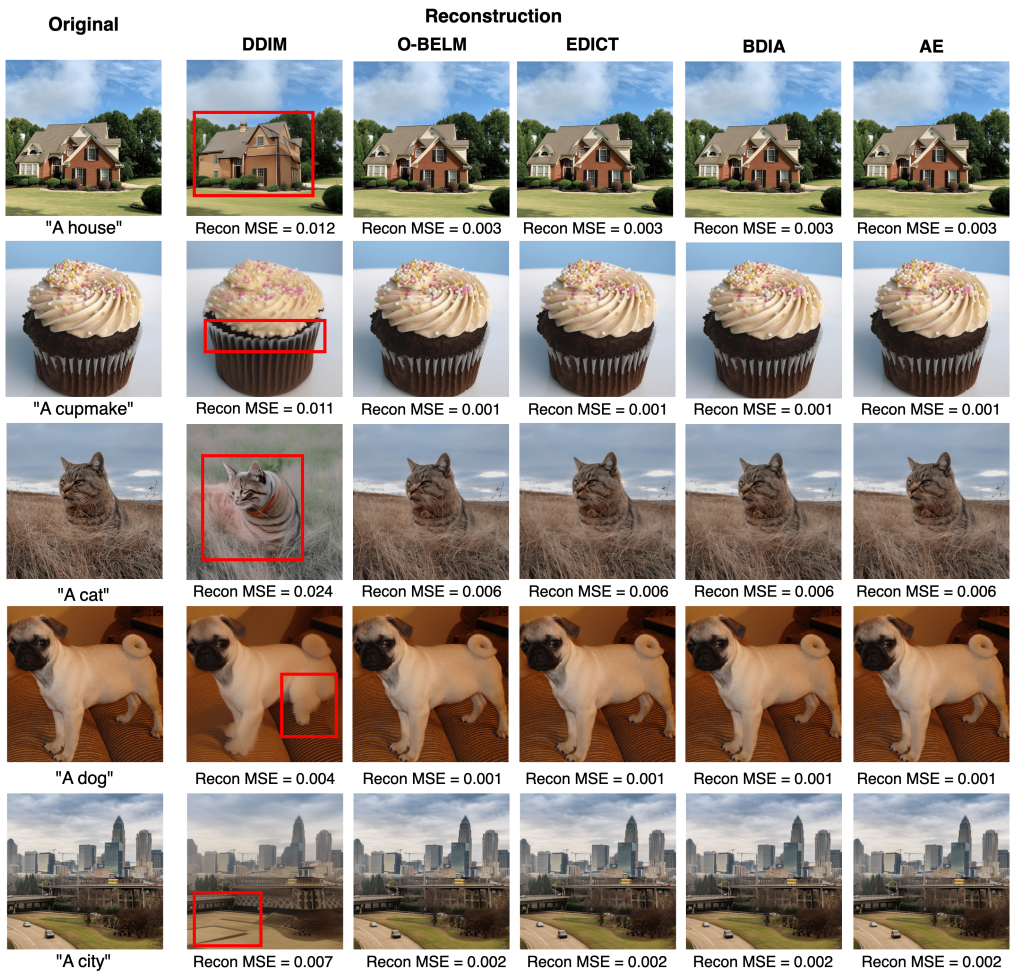

Figure 4: Results of image reconstruction and MSE error using DDIM and exact inversion samplers under 50 steps. The red rectangle point out the inconsistent part in the reconstructed images of DDIM.

C.2 Image Generation Results

hyperparameter choosing for EDICT and BDIA For EDICT and BDIA, each has an additional hyperparameter (γ and p respectively) whose optimal values are sensitive to the task at hand. To ascertain their appropriate hyperparameters for CIFAR-10 and CelebA-HQ, we executed a grid search in the 10-step scenario, as depicted in Table 6 and Table 7. These values were then fixed when performing cases with more steps. We evaluated γ in BDIA from 0 to 1 with a grid increment of 0.1, and assessed p in EDICT from 0.90 to 0.97 with a grid increment of 0.01, adhering to their suggested hyperparameter intervals. For the text-guided generation task using COCO-14 captions, we employed the values recommended in their respective papers.

Guidance Weight in Conditional Generation The 30k prompts is randomly selected from the COCO dataset [35] as the test set. For the text-guided generation task, we utilize a classifier-free

Table 6: Comparison of FID score($\downarrow$) of BDIA method for the task of CIFAR10/CelebA-HQ generation with different choice of γ in the 10-step scenario.

BDIA	The choice of γ										
	0.0	0.1	0.2	0.3	0.4	0.5	0.6	0.7	0.8	0.9	1.0
CIFAR10	17.41	**12.27**	15.60	23.62	33.39	43.93	54.93	66.32	78.33	92.16	106.37
CelebA-HQ	**27.41**	29.52	41.66	52.56	61.19	68.94	76.31	83.53	91.18	98.95	106.24

Table 7: Comparison of FID score($\downarrow$) of EDICT method for the task of CIFAR10/CelebA-HQ generation with different choice of p in the 10-step scenario.

EDICT	The choice of p							
	0.90	0.91	0.92	0.93	0.94	0.95	0.96	0.97
CIFAR10: 10 steps	149.00	142.81	135.05	127.52	119.57	110.50	99.86	**87.11**
CelebA-HQ: 10 steps	82.16	78.09	74.10	70.18	66.61	63.16	60.43	**57.82**

technique [22] which requires a guidance weight. For BDIA, we select a guidance weight of 4.0 and for EDICT, we choose 3.0, as recommended in their respective papers. For DDIM, we perform a grid search in the 20-step scenario, as shown in Table 8, and determine the optimal guidance weight to be 5.5. This value is then fixed for other scenarios as well as for the O-BELM sampler.

Table 8: Comparison of FID score($\downarrow$) of DDIM method for the task of text-guided generation with different choice of guidance weight.

DDIM	The choice of guidance weight										
	2.5	3.0	3.5	4.0	4.5	5.0	5.5	6.0	6.5	7.0	7.5
COCO-14	26.03	22.66	20.90	20.14	19.66	19.47	**19.45**	19.47	19.61	19.81	19.97

Examples of O-BELM We present unconditionally generated samples of O-BELM sampler in Figure 5(a) (CIFAR10, 32×32) and Figure 5(b) (CelebA-HQ, 256×256). Furthermore, we display text-guided generated samples in Figure 6, utilizing the pretrained SD-1.5 model [48] (512×512) with captions from the COCO-14 dataset [35]. The guidance weight for our O-BELM has been set at 5.5 to align with the choice of DDIM.

C.3 Image Interpolation

Image interpolation refers to the process of morphing between two images by interpolating between their corresponding latent vectors in the latent space, usually expecting to achieve a smooth transition between these images.

The diffusion ODE (5) establishes a correspondence between latent noise and samples, which can also be perceived as a coding for the samples. Given that O-BELM can more effectively simulate the diffusion ODE while preserving the one-to-one relationship of the coding, we believe that the exact inversion of O-BELM can intrinsically provide a more rational correspondence. This, in turn, facilitates superior interpolation effects.

We follow the experiment setting in [53] to generate interpolations on a line, which randomly sample two initial values $x_T^{(0)}$ and $x_T^{(1)}$ from the standard Gaussian $\mathcal{N}(0, 1)$, interpolate them with spherical linear interpolation [51], then use the BELM to obtain x_0 samples. The spherical linear interpolation $x_T^{(\alpha)}$ is calculated by

$$\mathbf{x}_T^{(\alpha)} = \frac{\sin((1-\alpha)\theta)}{\sin(\theta)}\mathbf{x}_T^{(0)} + \frac{\sin(\alpha\theta)}{\sin(\theta)}\mathbf{x}_T^{(1)}, \tag{64}$$

where $\theta = \arccos\left(\frac{\left(\mathbf{x}_T^{(0)}\right)^T\left(\mathbf{x}_T^{(1)}\right)}{\left\|\mathbf{x}_T^{(0)}\right\|\left\|\mathbf{x}_T^{(1)}\right\|}\right)$. We demonstrate the interpolation results of various models including CelebA-HQ (a), Butterflies (b), Emoji (c) and Anime (d) in Figure 7.

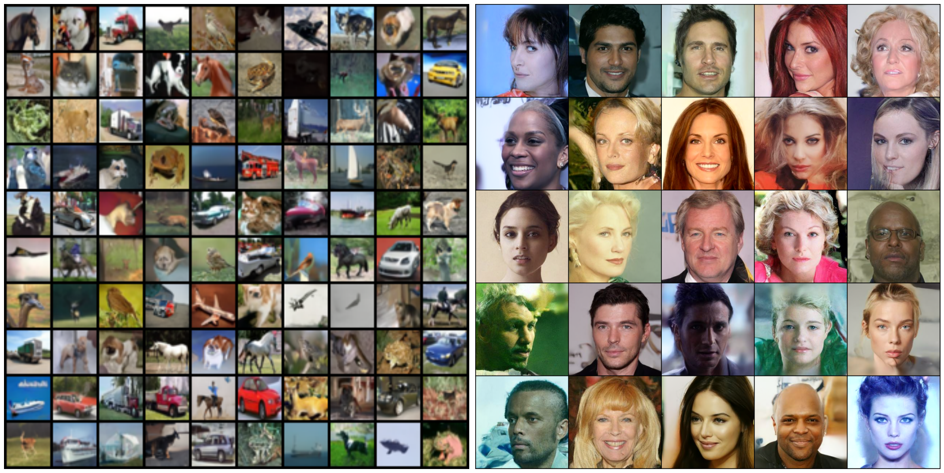

(a) (b)

Figure 5: (a) uncurated CIFAR10 samples with BELM, steps = 100 (b) uncurated CelebA-HQ samples with BELM, steps = 100

C.4 Image Editing

We adhere to the experimental setup of [63], initially introducing inversion noise to the images while preserving 20 percent of the steps during the inversion process. We utilize new prompts to reconstruct and edit the images. The guidance weight is consistently set at 3.0 for all instances.

C.4.1 ControlNet-Based Image Editing

We evaluated O-BELM and baseline algorithms on ControlNet-based image editing tasks, which included canny-based and depth-map-based editing as illustrated in Figure 8. The editing hyperparameters are chosen the same as our original paper. The ControlNet hyperparameters were kept at their default values, consistent across all methods. We set the number of steps to 100. The canny images were obtained using the Canny function from the opencv-python library, and the depth-map model used was Intel/dpt-large (`https://huggingface.co/Intel/dpt-large`). We use stable-diffusion-v1-5 model (`https://huggingface.co/runwayml/stable-diffusion-v1-5`) as our base model.

C.4.2 Style Transfer

We evaluated O-BELM and baseline algorithms on style transfer tasks using the style transfer sub-dataset of the PIE-Bench dataset (`https://paperswithcode.com/dataset/pie-bench`) as illustrated in Figure 9. The editing hyperparameters were selected to match those in our original paper. We use stable-diffusion-2-base model (`https://huggingface.co/stabilityai/stable-diffusion-2`) as our base model.

C.5 Pretrained Models

All of the pretrained models used in our research are open-sourced and available online as follows:

- CIFAR10 generation : ddpm_ema_cifar10
  https://github.com/VainF/Diff-Pruning/releases/download/v0.0.1/ddpm_ema_cifar10.zip
- CelebA-HQ generation and interpolation : ddpm-ema-celebahq-256
  https://huggingface.co/google/ddpm-ema-celebahq-256
- Text-to-Image generation : stable-diffusion-v1-5, stable-diffusion-2-base
  https://huggingface.co/runwayml/stable-diffusion-v1-5
  https://huggingface.co/stabilityai/stable-diffusion-2-base

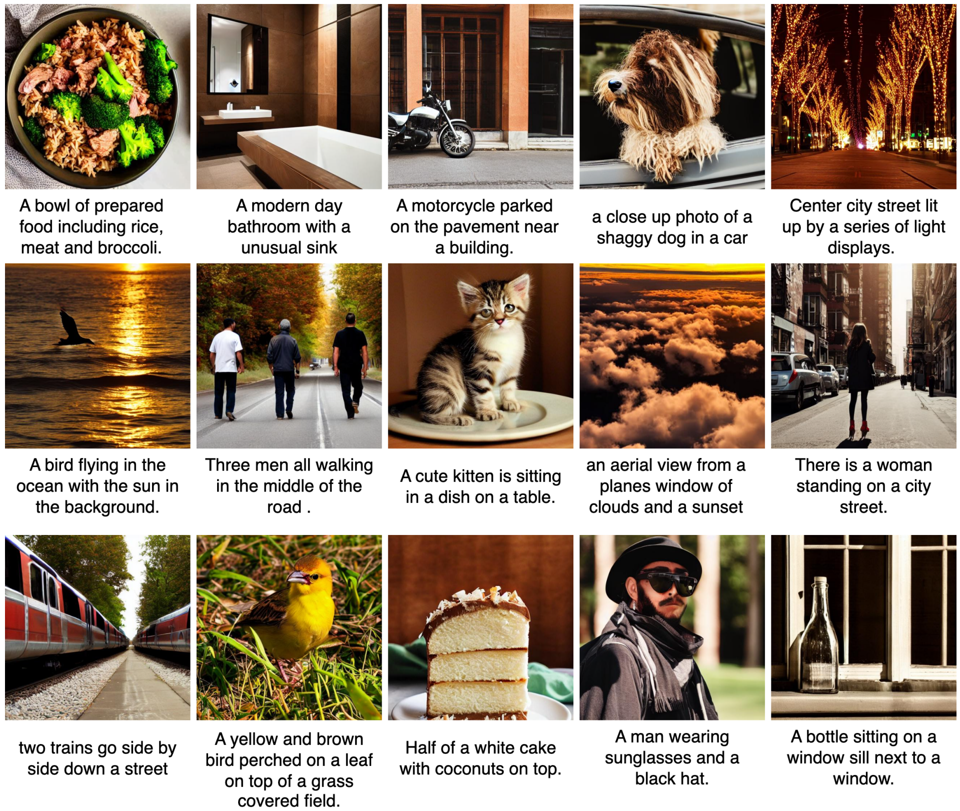

Figure 6: Prompts and generated images by O-BELM on COCO-14 dataset using SD-1.5 with 100 steps.

- Butterflies interpolation : ddim-butterflies-128
  https://huggingface.co/dboshardy/ddim-butterflies-128
- Emoji interpolation : ddpm-EmojiAlignedFaces-64
  https://huggingface.co/Norod78/ddpm-EmojiAlignedFaces-64
- Anime interpolation : ddpm-ema-anime-256
  https://huggingface.co/mrm8488/ddpm-ema-anime-256

The scheduler setting For these pre-trained diffusion models, we adopt the noise scheduler outlined in their respective configurations and apply it consistently across all our experiments. As our experiments do not involve the training or fine-tuning of diffusion models, there is no requirement to develop a new scheduler setting.

D Discussions

D.1 Hyperparameters of BDIA and EDICT

Notice that, the intuitive exact inversion samplers achieve exact diffusion inversion at a cost of introducing an additional hyperparameter. comparing to DDIM, including both BDIA (10) (with additional hyperparameter γ) and EDICT (9) (with additional hyperparameter p). We point out that the need for additional hyperparameters would hinder the widespread application of the exact inversion samplers. The sampling quality of the previous exact inversion samplers is highly inrobust to the additional hyperparameter. EDICT recommend to choose $p \in [0.9, 0.97]$ as EDICT would result in inconvergence when $p \leq 0.9$.

As depicted in Figure 10, we observe that the use of different hyperparameters within the recommended interval could potentially result in divergence. In Table 6 and Table 7, we note that the Frechet

(a) Interpolation Results on CelebA-HQ

(b) Interpolation Results on Butterflies

(c) Interpolation Results on Emoji

(d) Interpolation Results on Anime

Figure 7: Interpolation of samples of various models using O-BELM with 100 steps.

Inception Distance (FID) fluctuates significantly with respect to these unstable hyperparameters. Furthermore, the optimal hyperparameters vary across different datasets and steps.

D.2 The Different Definition on LTE

We would like to draw our readers' attention to the fact that the term Local Truncation Error (LTE) as used in this paper might differ from its usage in some other mathematical papers [58, p.317(12.24)]. Specifically, what is referred to as τ_i/h_i in this paper is often called LTE in other contexts, implying that their definition of LTE includes an additional division by a stepsize. However, in the context of variable-stepsize-variable-formula (VSVF), our definition proves to be more convenient and is more commonly adopted in papers dealing with VSVF [8, (2.1)].

D.3 Time Complexity and Memory Complexity

Time complexity Regarding the sampling task of diffusion models, the time cost bottleneck is the access to the noise network $\varepsilon_\theta(\mathbf{x}_i, i)$. The number of accesses to $\varepsilon_\theta(\mathbf{x}_i, i)$ is also referred to as NFE (the number of function evaluations). For the same value of N, we observed that O-BELM, DDIM, and BDIA all require an NFE equal to N for a single sampling chain. However, EDICT doubles this requirement to $2N$.

Experimentally, we've conducted additional tests to compare the average time cost of different methods across sampling, editing, and reconstruction tasks. The results show that O-BELM does

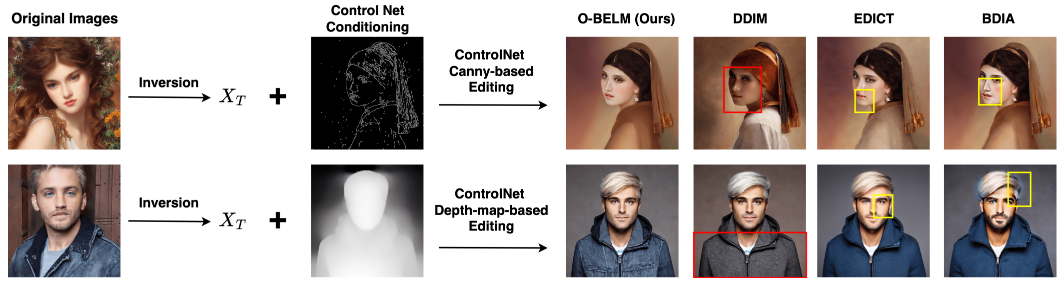

Figure 8: Comparison of ControlNet-based editing results of different samplers. DDIM leads to inconsistencies (red rectangle), and the EDICT and BDIA samplers introduce low-quality sections (yellow rectangle). Our O-BELM sampler ensures consistency and demonstrates high-quality results, even in such large scale editing and still preserve features from original images (face in the first example and clothing in the second example).

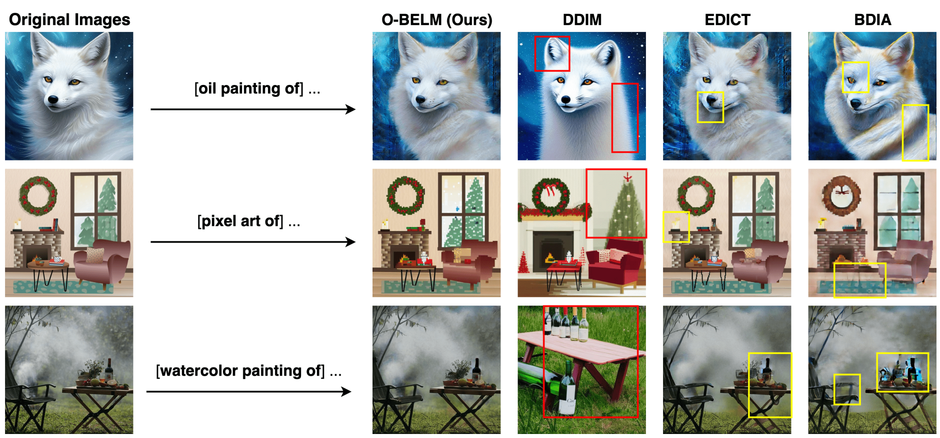

Figure 9: Comparison of Style Transfer results of different samplers on the PIE Benchmark. DDIM leads to inconsistencies (red rectangle), and the EDICT and BDIA samplers introduce low-quality sections (yellow rectangle). Our O-BELM sampler ensures structure preservation and high-quality style transfer, thus show the robustness and effectiveness of O-BELM sampler.

not incur any additional computational overhead compared to DDIM across all these tasks. Detailed information about these experiments can be found in Table 9.

Memory complexity During the sampling process of diffusion models, typically the entire chain of the process is maintained. Both BDIA and O-BELM do not require additional memory beyond the previous sampling path. However, due to the auxiliary states, the memory requirements of EDICT need to be doubled.

All experiments were conducted on a single V100 GPU and an Intel Xeon Platinum 8255C CPU. The sampling of 30k images using SD models under 100 steps took approximately 24 hours. The sampling of 50k images using a pre-trained CIFAR10 model under 100 steps took around 4 hours. Meanwhile, the sampling of 50k images using a pre-trained CelebA-HQ model under 100 steps required about 40 hours.

D.4 Other Inversion Techniques

We observe that the field of diffusion inversion is rapidly evolving. Recently, several works related to diffusion inversion have been proposed.

For instance, the study by [26] suggests altering the prior distribution, as opposed to using Gaussian noise, for more convenient inversion. However, this approach requires training new models, rendering it incompatible with existing pretrained models.

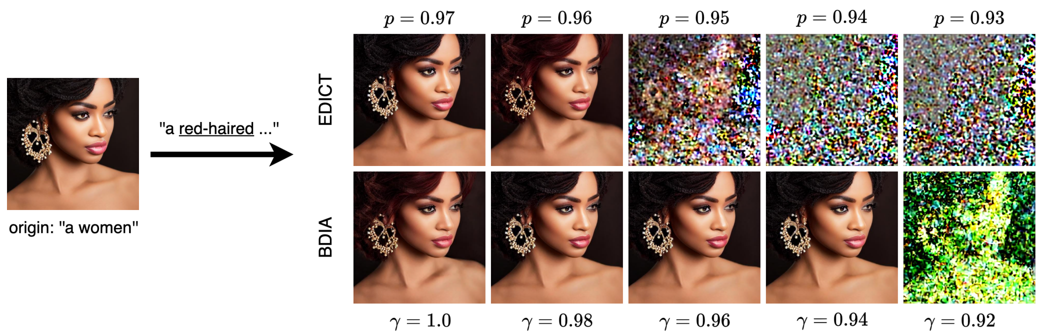

Figure 10: Image editing example for EDICT and BDIA with different hyperparameters, carried out over 200 steps. We observe that even within the interval advised in the original paper, the editing result may still diverge.

	Time costs of Different Tasks (50 steps)		
	Image Generation (s)	Image Editing (s)	Image Reconstruction (s)
DDIM	6.67	13.30	13.20
EDICT	12.67	25.77	25.72
BDIA	6.59	13.37	13.28
O-BELM(Ours)	**6.53**	**13.22**	**13.20**

Table 9: Comparison of time costs for different methods on the PIE Benchmark using the SD-2b model, as tested on a single NVIDIA Tesla V100. The results indicate that O-BELM does not incur additional computational time costs compared to DDIM across Generation, Editing, and Reconstruction tasks. We assessed the time costs of O-BELM and baseline algorithms using the PIE-Bench dataset (`https://paperswithcode.com/dataset/pie-bench`), which included tasks such as image generation, image editing, and image reconstruction. The number of steps was set to 50. We employed the stable-diffusion-2-base model (`https://huggingface.co/stabilityai/stable-diffusion-2`) as our base model and conducted tests on a single NVIDIA V100 chip and an Intel Xeon Platinum 8255C CPU.

The research conducted by [72, 16] advocates for the training of a model-dependent bias corrector for precise inversion. Despite this, it fails to achieve mathematically exact inversion.

The work of [39, 23] proposes the use of an implicit method in inversion to align with the sampling. However, this approach is time-consuming and residual optimization errors persist.

And, the study by [34] suggests training a reverse one-step consistency model. However, its experimental performance also demonstrates reconstruction inconsistency.

We understand that there are several techniques proposed to address the inexact inversion issue of DDIM within the context of *classifier-free-text-guided image editing*. These include NMG [5], DirectingInv [28], ProxEdit [17], NPT [41] and NT [42]. We point out that the proposed O-BELM and these techniques should not be considered as comparative algorithms for following reasons.

- These methods are orthogonal. O-BELM modifies the discretization formula to achieve exact inversion, while these techniques adjust the classifier-free-guidance mechanism. They address this problem from different directions.
- They can be used together in the classifier-free-text-guided image editing. Take DirectingInv as an instance, its inversion is just DDIM inversion and its forward process encompasses two state-interacting DDIM forward processes with different prompts. We can substitute the DDIM inversion/forward in DirectingInv to be O-BELM inversion/forward and get O-BELM+DirectingInv.
- Their working scenarios differ. The O-BELM is built on the general diffusion IVP, and can guarantee exact inversion and minimized error under all tasks based on diffusion ODE (PF-ODE). O-BELM can always converge to underlying IVP solution as demonstrated by

Proposition 5. This means that the BELM framework is compatible with a wide variety of diffusion-based tasks, irrespective of the data type (images or words), the task type (editing or interpolation), the guidance method (unconditional, classifier-free, classifier-based, or adjoint ODE-based), or the network structure (whether it includes an attention layer or not). On the contrary, these techniques are developed specific for classifier-free-text-guided image editing task.

D.5 Broader (Social) Impacts

The development of accurate and stable exact inversion diffusion sampling like O-BELM for DMs, as discussed in this paper, holds significant potential for several domains, including machine learning, healthcare, environmental modeling, and economics.

However, while this research holds great potential for positive impacts, it is also important to consider potential negative societal impacts. The enhanced ability of an accurate and stable exact diffusion sampler could potentially be misused. For instance, it could be exploited to creating deepfakes, leading to misinformation. It may also raise privacy concerns, as more detailed and source data can be decoded from the intermediates using O-BELM. In healthcare, if not properly regulated, the use of synthetic patient data could lead to ethical issues. Therefore, it is crucial to ensure that the findings of this research are applied ethically and responsibly, with necessary safeguards in place to prevent misuse and protect privacy.

D.6 Limitations

This paper does not explore the integration of high-accuracy exact inversion samplers such as O-BELM with more powerful image editing pipelines. Additionally, the application of high-accuracy exact inversion samplers like O-BELM to tasks beyond image processing remains uninvestigated in this work. The concept of employing bidirectional explicit constraints to ensure exact inversion when applied to accelerated DM-solvers remains unexplored. There is also a lot of downstream tasks of DMs that a exact inversion samplers like O-BELM can apply [64, 61, 60, 4, 66, 13, 59, 70, 15, 14]. It will be also interesting to apply the exact inversion ODE sampler in variational inference [69, 65] or flow matching [36, 76].

NeurIPS Paper Checklist

The checklist is designed to encourage best practices for responsible machine learning research, addressing issues of reproducibility, transparency, research ethics, and societal impact. Do not remove the checklist: **The papers not including the checklist will be desk rejected.** The checklist should follow the references and precede the (optional) supplemental material. The checklist does NOT count towards the page limit.

Please read the checklist guidelines carefully for information on how to answer these questions. For each question in the checklist:

- You should answer [Yes] , [No] , or [NA] .
- [NA] means either that the question is Not Applicable for that particular paper or the relevant information is Not Available.
- Please provide a short (1–2 sentence) justification right after your answer (even for NA).

The checklist answers are an integral part of your paper submission. They are visible to the reviewers, area chairs, senior area chairs, and ethics reviewers. You will be asked to also include it (after eventual revisions) with the final version of your paper, and its final version will be published with the paper.

The reviewers of your paper will be asked to use the checklist as one of the factors in their evaluation. While "[Yes] " is generally preferable to "[No] ", it is perfectly acceptable to answer "[No] " provided a proper justification is given (e.g., "error bars are not reported because it would be too computationally expensive" or "we were unable to find the license for the dataset we used"). In general, answering "[No] " or "[NA] " is not grounds for rejection. While the questions are phrased in a binary way, we acknowledge that the true answer is often more nuanced, so please just use your best judgment and write a justification to elaborate. All supporting evidence can appear either in the main paper or the supplemental material, provided in appendix. If you answer [Yes] to a question, in the justification please point to the section(s) where related material for the question can be found.

IMPORTANT, please:

- **Delete this instruction block, but keep the section heading "NeurIPS paper checklist"**,
- **Keep the checklist subsection headings, questions/answers and guidelines below.**
- **Do not modify the questions and only use the provided macros for your answers**.

1. **Claims**

   Question: Do the main claims made in the abstract and introduction accurately reflect the paper's contributions and scope?

   Answer: [Yes]

   Justification: Our main claims do reflect the theory and experiment contents of the paper.

   Guidelines:

   - The answer NA means that the abstract and introduction do not include the claims made in the paper.
   - The abstract and/or introduction should clearly state the claims made, including the contributions made in the paper and important assumptions and limitations. A No or NA answer to this question will not be perceived well by the reviewers.
   - The claims made should match theoretical and experimental results, and reflect how much the results can be expected to generalize to other settings.
   - It is fine to include aspirational goals as motivation as long as it is clear that these goals are not attained by the paper.

2. **Limitations**

   Question: Does the paper discuss the limitations of the work performed by the authors?

   Answer: [Yes]

   Justification: We discuss about the limitations of the work in Appendix D.4.

Guidelines:

- The answer NA means that the paper has no limitation while the answer No means that the paper has limitations, but those are not discussed in the paper.
- The authors are encouraged to create a separate "Limitations" section in their paper.
- The paper should point out any strong assumptions and how robust the results are to violations of these assumptions (e.g., independence assumptions, noiseless settings, model well-specification, asymptotic approximations only holding locally). The authors should reflect on how these assumptions might be violated in practice and what the implications would be.
- The authors should reflect on the scope of the claims made, e.g., if the approach was only tested on a few datasets or with a few runs. In general, empirical results often depend on implicit assumptions, which should be articulated.
- The authors should reflect on the factors that influence the performance of the approach. For example, a facial recognition algorithm may perform poorly when image resolution is low or images are taken in low lighting. Or a speech-to-text system might not be used reliably to provide closed captions for online lectures because it fails to handle technical jargon.
- The authors should discuss the computational efficiency of the proposed algorithms and how they scale with dataset size.
- If applicable, the authors should discuss possible limitations of their approach to address problems of privacy and fairness.
- While the authors might fear that complete honesty about limitations might be used by reviewers as grounds for rejection, a worse outcome might be that reviewers discover limitations that aren't acknowledged in the paper. The authors should use their best judgment and recognize that individual actions in favor of transparency play an important role in developing norms that preserve the integrity of the community. Reviewers will be specifically instructed to not penalize honesty concerning limitations.

3. **Theory Assumptions and Proofs**

   Question: For each theoretical result, does the paper provide the full set of assumptions and a complete (and correct) proof?

   Answer: [Yes]

   Justification: For every theoretical result, we give the needed assumptions and proofs.

   Guidelines:

   - The answer NA means that the paper does not include theoretical results.
   - All the theorems, formulas, and proofs in the paper should be numbered and cross-referenced.
   - All assumptions should be clearly stated or referenced in the statement of any theorems.
   - The proofs can either appear in the main paper or the supplemental material, but if they appear in the supplemental material, the authors are encouraged to provide a short proof sketch to provide intuition.
   - Inversely, any informal proof provided in the core of the paper should be complemented by formal proofs provided in appendix or supplemental material.
   - Theorems and Lemmas that the proof relies upon should be properly referenced.

4. **Experimental Result Reproducibility**

   Question: Does the paper fully disclose all the information needed to reproduce the main experimental results of the paper to the extent that it affects the main claims and/or conclusions of the paper (regardless of whether the code and data are provided or not)?

   Answer: [Yes]

   Justification: Our dataset, parameters and code will be uploaded to ensure reproducibility.

   Guidelines:

   - The answer NA means that the paper does not include experiments.

- If the paper includes experiments, a No answer to this question will not be perceived well by the reviewers: Making the paper reproducible is important, regardless of whether the code and data are provided or not.
- If the contribution is a dataset and/or model, the authors should describe the steps taken to make their results reproducible or verifiable.
- Depending on the contribution, reproducibility can be accomplished in various ways. For example, if the contribution is a novel architecture, describing the architecture fully might suffice, or if the contribution is a specific model and empirical evaluation, it may be necessary to either make it possible for others to replicate the model with the same dataset, or provide access to the model. In general. releasing code and data is often one good way to accomplish this, but reproducibility can also be provided via detailed instructions for how to replicate the results, access to a hosted model (e.g., in the case of a large language model), releasing of a model checkpoint, or other means that are appropriate to the research performed.
- While NeurIPS does not require releasing code, the conference does require all submissions to provide some reasonable avenue for reproducibility, which may depend on the nature of the contribution. For example
  (a) If the contribution is primarily a new algorithm, the paper should make it clear how to reproduce that algorithm.
  (b) If the contribution is primarily a new model architecture, the paper should describe the architecture clearly and fully.
  (c) If the contribution is a new model (e.g., a large language model), then there should either be a way to access this model for reproducing the results or a way to reproduce the model (e.g., with an open-source dataset or instructions for how to construct the dataset).
  (d) We recognize that reproducibility may be tricky in some cases, in which case authors are welcome to describe the particular way they provide for reproducibility. In the case of closed-source models, it may be that access to the model is limited in some way (e.g., to registered users), but it should be possible for other researchers to have some path to reproducing or verifying the results.

5. **Open access to data and code**

   Question: Does the paper provide open access to the data and code, with sufficient instructions to faithfully reproduce the main experimental results, as described in supplemental material?

   Answer: [Yes]

   Justification: The dataset utilized in this paper is publicly accessible on the internet. We have included codes, along with corresponding instructions, in the supplementary materials and intend to make them available on GitHub. However, our Stable Diffusion-related code is deeply intertwined with our proprietary business code, and we are currently working on decoupling the codebase. As soon as this process is complete, we will make them available on GitHub.

   Guidelines:

   - The answer NA means that paper does not include experiments requiring code.
   - Please see the NeurIPS code and data submission guidelines (`https://nips.cc/public/guides/CodeSubmissionPolicy`) for more details.
   - While we encourage the release of code and data, we understand that this might not be possible, so "No" is an acceptable answer. Papers cannot be rejected simply for not including code, unless this is central to the contribution (e.g., for a new open-source benchmark).
   - The instructions should contain the exact command and environment needed to run to reproduce the results. See the NeurIPS code and data submission guidelines (`https://nips.cc/public/guides/CodeSubmissionPolicy`) for more details.
   - The authors should provide instructions on data access and preparation, including how to access the raw data, preprocessed data, intermediate data, and generated data, etc.

- The authors should provide scripts to reproduce all experimental results for the new proposed method and baselines. If only a subset of experiments are reproducible, they should state which ones are omitted from the script and why.
- At submission time, to preserve anonymity, the authors should release anonymized versions (if applicable).
- Providing as much information as possible in supplemental material (appended to the paper) is recommended, but including URLs to data and code is permitted.

6. **Experimental Setting/Details**

   Question: Does the paper specify all the training and test details (e.g., data splits, hyper-parameters, how they were chosen, type of optimizer, etc.) necessary to understand the results?

   Answer: [Yes]

   Justification: We provide the details of our experiments in Appendix C.

   Guidelines:

   - The answer NA means that the paper does not include experiments.
   - The experimental setting should be presented in the core of the paper to a level of detail that is necessary to appreciate the results and make sense of them.
   - The full details can be provided either with the code, in appendix, or as supplemental material.

7. **Experiment Statistical Significance**

   Question: Does the paper report error bars suitably and correctly defined or other appropriate information about the statistical significance of the experiments?

   Answer: [NA]

   Justification: This paper does not raise any issues related to statistical significance.

   Guidelines:

   - The answer NA means that the paper does not include experiments.
   - The authors should answer "Yes" if the results are accompanied by error bars, confidence intervals, or statistical significance tests, at least for the experiments that support the main claims of the paper.
   - The factors of variability that the error bars are capturing should be clearly stated (for example, train/test split, initialization, random drawing of some parameter, or overall run with given experimental conditions).
   - The method for calculating the error bars should be explained (closed form formula, call to a library function, bootstrap, etc.)
   - The assumptions made should be given (e.g., Normally distributed errors).
   - It should be clear whether the error bar is the standard deviation or the standard error of the mean.
   - It is OK to report 1-sigma error bars, but one should state it. The authors should preferably report a 2-sigma error bar than state that they have a 96% CI, if the hypothesis of Normality of errors is not verified.
   - For asymmetric distributions, the authors should be careful not to show in tables or figures symmetric error bars that would yield results that are out of range (e.g. negative error rates).
   - If error bars are reported in tables or plots, The authors should explain in the text how they were calculated and reference the corresponding figures or tables in the text.

8. **Experiments Compute Resources**

   Question: For each experiment, does the paper provide sufficient information on the computer resources (type of compute workers, memory, time of execution) needed to reproduce the experiments?

   Answer: [Yes]

   Justification: We do provide sufficient information on the computer resources in Appendix D.3.

Guidelines:

- The answer NA means that the paper does not include experiments.
- The paper should indicate the type of compute workers CPU or GPU, internal cluster, or cloud provider, including relevant memory and storage.
- The paper should provide the amount of compute required for each of the individual experimental runs as well as estimate the total compute.
- The paper should disclose whether the full research project required more compute than the experiments reported in the paper (e.g., preliminary or failed experiments that didn't make it into the paper).

9. **Code Of Ethics**

   Question: Does the research conducted in the paper conform, in every respect, with the NeurIPS Code of Ethics `https://neurips.cc/public/EthicsGuidelines`?

   Answer: [Yes]

   Justification: This paper do conform with the NeurIPS Code of Ethics.

   Guidelines:

   - The answer NA means that the authors have not reviewed the NeurIPS Code of Ethics.
   - If the authors answer No, they should explain the special circumstances that require a deviation from the Code of Ethics.
   - The authors should make sure to preserve anonymity (e.g., if there is a special consideration due to laws or regulations in their jurisdiction).

10. **Broader Impacts**

    Question: Does the paper discuss both potential positive societal impacts and negative societal impacts of the work performed?

    Answer: [Yes]

    Justification: We talk about the potential societal impacts in Appendix D.5.

    Guidelines:

    - The answer NA means that there is no societal impact of the work performed.
    - If the authors answer NA or No, they should explain why their work has no societal impact or why the paper does not address societal impact.
    - Examples of negative societal impacts include potential malicious or unintended uses (e.g., disinformation, generating fake profiles, surveillance), fairness considerations (e.g., deployment of technologies that could make decisions that unfairly impact specific groups), privacy considerations, and security considerations.
    - The conference expects that many papers will be foundational research and not tied to particular applications, let alone deployments. However, if there is a direct path to any negative applications, the authors should point it out. For example, it is legitimate to point out that an improvement in the quality of generative models could be used to generate deepfakes for disinformation. On the other hand, it is not needed to point out that a generic algorithm for optimizing neural networks could enable people to train models that generate Deepfakes faster.
    - The authors should consider possible harms that could arise when the technology is being used as intended and functioning correctly, harms that could arise when the technology is being used as intended but gives incorrect results, and harms following from (intentional or unintentional) misuse of the technology.
    - If there are negative societal impacts, the authors could also discuss possible mitigation strategies (e.g., gated release of models, providing defenses in addition to attacks, mechanisms for monitoring misuse, mechanisms to monitor how a system learns from feedback over time, improving the efficiency and accessibility of ML).

11. **Safeguards**

    Question: Does the paper describe safeguards that have been put in place for responsible release of data or models that have a high risk for misuse (e.g., pretrained language models, image generators, or scraped datasets)?

Answer: [NA]

Justification: We do not release anything that carries a high risk of misuse.

Guidelines:

- The answer NA means that the paper poses no such risks.
- Released models that have a high risk for misuse or dual-use should be released with necessary safeguards to allow for controlled use of the model, for example by requiring that users adhere to usage guidelines or restrictions to access the model or implementing safety filters.
- Datasets that have been scraped from the Internet could pose safety risks. The authors should describe how they avoided releasing unsafe images.
- We recognize that providing effective safeguards is challenging, and many papers do not require this, but we encourage authors to take this into account and make a best faith effort.

12. **Licenses for existing assets**

    Question: Are the creators or original owners of assets (e.g., code, data, models), used in the paper, properly credited and are the license and terms of use explicitly mentioned and properly respected?

    Answer: [Yes]

    Justification: All such assets are appropriately credited, and the license and terms of use are explicitly mentioned and duly respected.

    Guidelines:

    - The answer NA means that the paper does not use existing assets.
    - The authors should cite the original paper that produced the code package or dataset.
    - The authors should state which version of the asset is used and, if possible, include a URL.
    - The name of the license (e.g., CC-BY 4.0) should be included for each asset.
    - For scraped data from a particular source (e.g., website), the copyright and terms of service of that source should be provided.
    - If assets are released, the license, copyright information, and terms of use in the package should be provided. For popular datasets, `paperswithcode.com/datasets` has curated licenses for some datasets. Their licensing guide can help determine the license of a dataset.
    - For existing datasets that are re-packaged, both the original license and the license of the derived asset (if it has changed) should be provided.
    - If this information is not available online, the authors are encouraged to reach out to the asset's creators.

13. **New Assets**

    Question: Are new assets introduced in the paper well documented and is the documentation provided alongside the assets?

    Answer: [NA]

    Justification: We do not introduce new assets.

    Guidelines:

    - The answer NA means that the paper does not release new assets.
    - Researchers should communicate the details of the dataset/code/model as part of their submissions via structured templates. This includes details about training, license, limitations, etc.
    - The paper should discuss whether and how consent was obtained from people whose asset is used.
    - At submission time, remember to anonymize your assets (if applicable). You can either create an anonymized URL or include an anonymized zip file.

14. **Crowdsourcing and Research with Human Subjects**

Question: For crowdsourcing experiments and research with human subjects, does the paper include the full text of instructions given to participants and screenshots, if applicable, as well as details about compensation (if any)?

Answer: [NA]

Justification: This paper do not involve Human participants.

Guidelines:

- The answer NA means that the paper does not involve crowdsourcing nor research with human subjects.
- Including this information in the supplemental material is fine, but if the main contribution of the paper involves human subjects, then as much detail as possible should be included in the main paper.
- According to the NeurIPS Code of Ethics, workers involved in data collection, curation, or other labor should be paid at least the minimum wage in the country of the data collector.

15. **Institutional Review Board (IRB) Approvals or Equivalent for Research with Human Subjects**

Question: Does the paper describe potential risks incurred by study participants, whether such risks were disclosed to the subjects, and whether Institutional Review Board (IRB) approvals (or an equivalent approval/review based on the requirements of your country or institution) were obtained?

Answer: [NA]

Justification: This paper do not involve Human participants.

Guidelines:

- The answer NA means that the paper does not involve crowdsourcing nor research with human subjects.
- Depending on the country in which research is conducted, IRB approval (or equivalent) may be required for any human subjects research. If you obtained IRB approval, you should clearly state this in the paper.
- We recognize that the procedures for this may vary significantly between institutions and locations, and we expect authors to adhere to the NeurIPS Code of Ethics and the guidelines for their institution.
- For initial submissions, do not include any information that would break anonymity (if applicable), such as the institution conducting the review.